SANDIA REPORT

SAND95–1706 •• UC–406

Unlimited Release

Printed August 1995

Intelligent Systems for Induction Hardening Processes

(24 Month Report)

Douglas R. Adkins, J. Bruce Kelley, Phil M. Kahle, Charles V. Robino, Suzanne L. Stanton, David K. Gartling, Russell D. Skocypec, Gerald A. Knorovsky

Prepared by
Sandia National Laboratories
Albuquerque, New Mexico 87185 and Livermore, California 94550
for the United States Department of Energy
under Contract DE-AC04-94AL85000

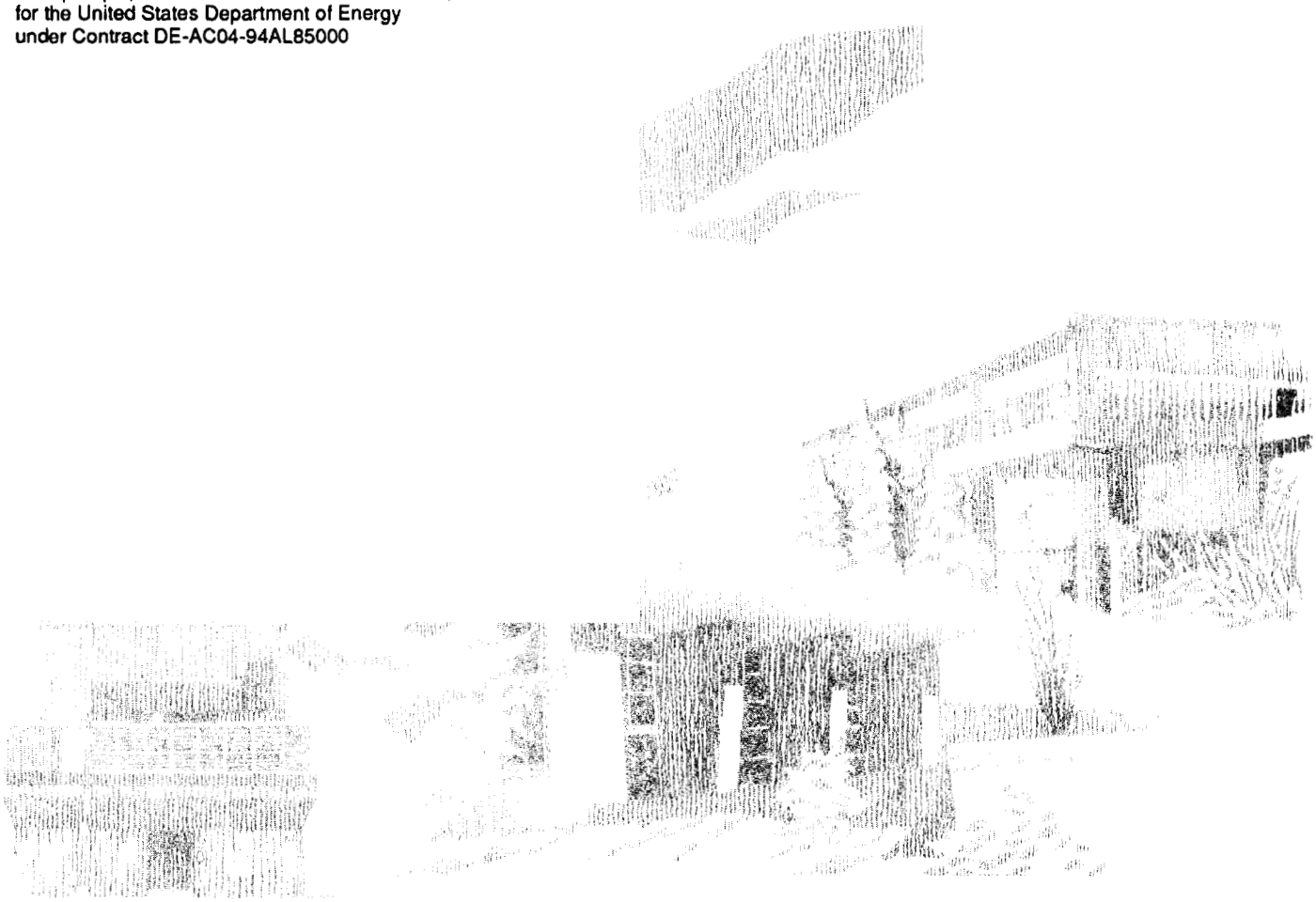

SF2900Q(8-81)

44P.

Issued by Sandia National Laboratories, operated for the United States Department of Energy by Sandia Corporation.

SAND95–1706
Unlimited Release
Printed August 1995

Distribution
Category UC–406

Intelligent Systems for Induction Hardening Processes (24 Month Report)

Douglas R. Adkins, J. Bruce Kelley, Phil M. Kahle,
Charles V. Robino, Suzanne L. Stanton, David K. Gartling,
Russell D. Skocypec, Gerald A. Knorovsky
Thermal and Fluid Engineering Department
Sandia National Laboratories
Albuquerque, NM 87185

ABSTRACT

General Motors' Delphi Saginaw Steering System and Sandia National Laboratories are working through a Cooperative Research and Development Agreement (CRADA) to develop real-time process controls for induction hardening systems and develop a better fundamental understanding of the induction heating process as related to materials and other process variables. The program consists of four tasks: (1) Process Characterization, (2) Data Acquisition and Controller Development, (3) Material Characterization, and (4) Computational Modeling. In the first year of this program a technical base was established in each of these areas that allowed us to understand the induction heating process and to identify the best approach to control the process in a laboratory environment. The second year of this program was dedicated to implementing this knowledge to control the induction heating process in the laboratory environment and to begin developing the hardware and software needed for control on the factory floor. Accomplishments in the first two years of this program will enable us to move this control technology to the factory floor in the third year of this CRADA.

Intentionally Left Blank

CONTENTS

Figures

Figures (continued)

Tables

EXECUTIVE SUMMARY

Induction hardening is widely used to provide enhanced strength, wear resistance, and toughness in components made from medium and high carbon steels. Current limitations of the process include the lack of closed-loop process control, previously unidentified process and material variations which cause continual adjustment of the process parameters, coil and process development by trial and error, and an inability to monitor coil condition. Improvement of the induction hardening process is limited by an inadequate understanding of process fundamentals and material/process interactions.

A multidisciplinary team from Sandia National Laboratories and Delphi Saginaw Steering Systems is investigating the induction hardening process under a Cooperative Research and Development Agreement (CRADA). Delphi Saginaw Steering Systems is a wholly owned subsidiary of General Motors. The program consists of four Tasks: (1) Process Characterization, (2) Materials Characterization, (3) Computational Modeling, and (4) Data Acquisition and Control. The primary goal for the first year of this program was to establish a technical base in each of these areas that will allow us to understand the induction heating process and to identify the best approach to control the process in a laboratory environment. The second year of this program was dedicated to implementing this knowledge to control the induction heating process in the laboratory environment and to begin developing the hardware and software needed for control on the factory floor. In the third and final year of this program, the control system will be introduced to the factory floor, and the knowledge and computational tools developed will be fully transferred to Saginaw.

During the last 12 months, a number of prototype monitors and controllers were evaluated at Sandia. A first generation neural network controller was demonstrated at Sandia and in the induction laboratory at Delphi Saginaw. The application of intelligent control algorithms has led to the development of a closed-loop process controller that controls the HRC 50 case thickness to $\pm$ 0.1 mm for the combination of one material and one geometry in a single-shot process. *This controller system uses a unique signal processing algorithm that computes the power delivered to the part during the heating process.* Physical changes in the part are reflected in this signal. Other highlights from the past year include:

- Incorporated heat-to-heat material variations in neural network control.
- Collected data streams for scanning induction systems at Saginaw to explore the possibility of controlling a wider variety of induction machines with a neural network system.
- Stockpiled production materials were characterized to assess the impact of variations in carbon content, ideal diameter, and Jominy hardenability on the induction hardened product.
- Identified analysis techniques for austination kinetics to study the effect of the high heating rates of inductiuon systems on material phase transformations.
- Mapped variations in electromagnetic properties of production materials as a function of temperature and induction frequency.
- Completed parametric analysis with 1-D model that demonstrated the dominance of Curie temperature on process control.
- Continued development of 3-D induction heating model and conducted tests for model validation.

These accomplishments have positioned the program at a point where the third year goal of introducing the neural-network induction control system on the factory floor at Delphi Saginaw is achievable. Further work in computational modeling and materials characterization in the third and last year of the CRADA will also improve the application and understanding of this important idustrial heat treating process.

NOMENCLATURE

A = magnetic field potential, Wb/m
B = magnetic flux density, Wb/m^2
C = specific heat, kJ/kg K
E = electrical potential, V/m
H = magnetic field strength, A/m
H_s = saturation magnetic field strength, A/m
I = current in each circuit, A
J = current density, A/m^2
K = thermal conductivity of the part, W/m K
Q = power input from Joule heating, W/m^3
R = circuit resistance, ohms
V = applied voltage in each circuit, V
T = temperature, K
T_c = Curie temperature, K

f = frequency, Hz
h_c = hysteresis loss per cycle,

μ = magnetic permeability, Wb/A m
μ_o = magnetic constant, $4\pi x10^{-7}$ Wb/A m
μ_r = relative permeability at room temperature
ρ = density, kg/m^3
σ = electrical conductivity, mho/m

Intentionally Left Blank

Intelligent Systems for Induction Hardening Processes (24 Month Report)

INTRODUCTION

Induction hardening is widely used in the automotive, off-highway, and industrial equipment industries to provide enhanced strength, wear resistance, and toughness in components made from medium and high carbon steels [Zinn and Semiatin, 1988, Davies and Simpson, 1986, Tudbury, 1960, Kern and Suess, 1986]. Industrial equipment components such as ball screws, actuator shafts, wear pins, and valve seats are often induction hardened. Commonly hardened components in the automotive industry include drivetrain components such as axles, gears, and constant velocity joints; engine components such as crankshafts, camshafts, and pump shafts; and chassis components such as spindle bearings and steering racks. Delphi Saginaw Steering Systems, formerly Saginaw Division of General Motors, is one of the world's largest users of this technology, hardening such components as axle shafts, constant velocity joint races, pump shafts, drive shafts, and steering components. Nearly 250,000 parts are induction hardened daily by Delphi Saginaw at numerous locations in the United States and worldwide.

Induction hardening is extensively used because it is a very fast, energy efficient, in-line heat treating technology that applies energy only to the volume of material required to be hardened. Short treatment times and decreased distortion generally result in less scrap, rework, and post-heat-treatment machining of parts. Induction hardening is also an environmentally benign process, requiring no endothermic atmospheres, plating processes, or stripping tanks. In contrast, the primary competing heat treating technology, carburizing, is an off-line batch process in which the entire volume of material is heated in a furnace. Batch heat treating results in higher direct energy costs, longer manufacturing lead times, and greater amounts of distortion when parts are quenched [Storm and Chaplin, 1987]. In today's competitive environment, the ability to heat treat parts rapidly with in-line technology generates significant savings and quality improvements.

Despite these advantages, induction hardening is not as broadly used as it might be. The lack of closed-loop process control results in quality control by destructive evaluation, necessitating a high-cost infrastructure for high-volume, close-tolerance parts. Previously unidentified material and process variations cause continual adjustment of process parameters. Variability of the induction hardening process leads to variability in resulting part case depths and mechanical properties. Because coil and process development are experience-based, iterative procedures, tooling and process development are not often optimized. The associated lead times and uncertainties for coil and process development inhibit the use of induction hardening even when the potential payoff for use is high. These factors lead to wide process windows, frequent destructive inspection requirements, heavier parts due to lower allowable design stress limits, and higher-than-desirable reject rates.

A multidisciplinary team from Sandia National Labs and Delphi Saginaw Steering Systems was formed in February of 1993 to investigate the induction hardening process under a Cooperative Research and Development Agreement (CRADA). The team consists of scientists and engineers with expertise in the thermal and fluid sciences, materials and processes sciences, pulsed power physics, advanced manufacturing controls, and manufacturing engineering. The overall purpose of the project is to improve the fundamental understanding of the process and material/process interactions, and to apply intelligent manufacturing algorithms and control systems to the induction hardening process. The anticipated results include a closed-loop control algorithm or process monitor with embedded robust materials and process criteria to ensure consistent final products.

To achieve these goals, four interrelated areas of investigation were defined: (1) process characterization, (2) material characterization, (3) computational modeling, and (4) data acquisition and controller development. A program of coupled experimental and computational tasks conducted in multiple phases was defined to progressively move lab concepts to the factory floor. A specific part geometry and material (Saturn half shaft and 1050M steel) were selected to be representative of Saginaw processes and provide an accurate assessment of the potential to achieve closed-loop control.

PROCESS CHARACTERIZATION

Induction hardening of a steel part is accomplished by passing an alternating current through a water-cooled copper coil which is coupled to the part by the induced magnetic field as shown in Figure 1. The alternating magnetic field induces eddy currents which resistively heat the outer surface of the part. The part is then quenched when the austenitized layer reaches the desired thickness. Many process parameters and material properties affect the thermal response of the part, including the amplitude, frequency and wave shape of the applied voltage; part geometry and the coupling between the coil and part; the electromagnetic properties such as electrical conductivity and magnetic permeability which are functions of temperature and frequency; plus the thermophysical properties such as thermal conductivity and specific heat of transformation.

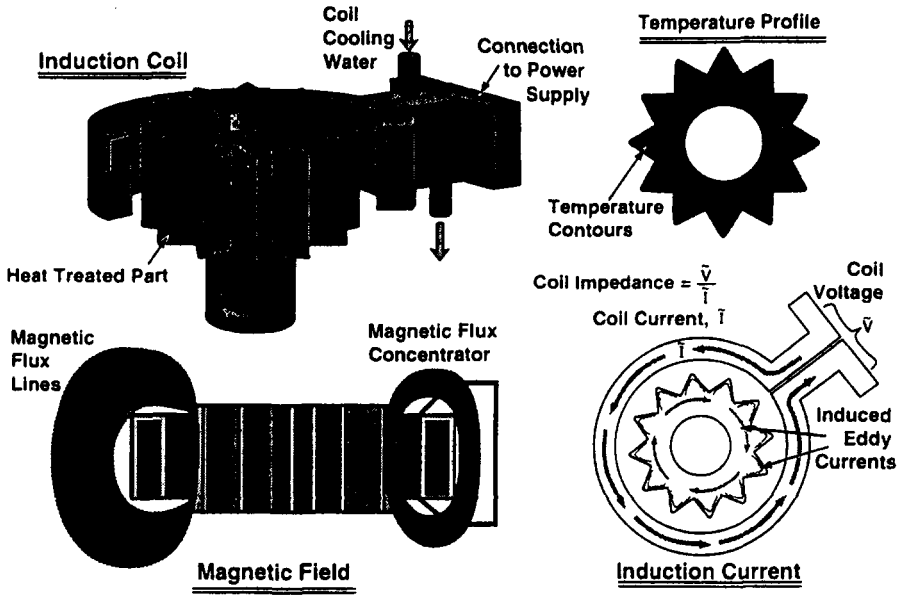

Figure 1. Schematic of the induction heating process. The part and coil are coupled through the magnetic field, enabling tracking of the process by monitoring the coil signals.

The goal of the process characterization task is to develop a noninvasive process signature to track the progress of the process and enable closed-loop control. Electrical signals were the primary focus of the task from the start because they are readily available in production equipment and are easily adapted for control purposes. The basis of the process characterization task is that the coil and part are integrally linked through the magnetic field so changes in the part properties which occur as a result of heating should be reflected in the coil signature [Zinn and Semiatin, 1988, Verhoeven et al, 1986, Mordwinkin et al, 1986, Hassel, 1986, 1994, Martin and Wiley, 1956]. The challenge is to understand and relate the electrical signal variations to the resultant case depth, defined for this project as the depth to 50 HRC.

Delphi Saginaw provided a 10 kHz, 100-kW single shot machine for experimentation at Sandia's facility in Albuquerque, New Mexico, along with the expertise of how heat treating is accomplished in an

industrial setting on a production line. Delphi Saginaw also provided test pieces which consisted of right circular cylinders and spline-end pieces cut from axle bars, along with a number of appropriate induction coils. Coil voltage and current monitoring devices were developed by Sandia for reliable operation in the high magnetic field environment around the induction coil. Additional machine functions were also instrumented to completely characterize machine operation and control functions. A 486 EISA-bus personal computer with a megahertz-speed data acquisition card was installed for collection and processing of the acquired signals.

During the first year of the project a unique signal processing algorithm was developed that separates the power and energy delivered to the part from the total power and energy delivered by the induction machine[Frost et al, 1994]. Experimental validation of the signal processing algorithm was achieved by using a specially fabricated specimen calorimeter and by using the induction coil as a calorimeter. Results from the signal processing algorithm were correlated with the computational model.

The signal processing algorithm provides a suite of 8 signals which change as the process progresses and vary across the parameter space of interest. As an example, the variation of one of the signals is shown for three different materials in Figure 2. As shown in the figure, the signal from IN 718, a paramagnetic material, stays constant through the heating cycle. The signal from AISI 1050, a ferromagnetic medium carbon steel, exhibits a peak in the signal about halfway through a heating cycle which resulted in a nominal case depth. A third material, Hiperco 50, a ferromagnetic material with a high curie temperature, also exhibited a peak in the signal but the peak occurred later in the cycle. The

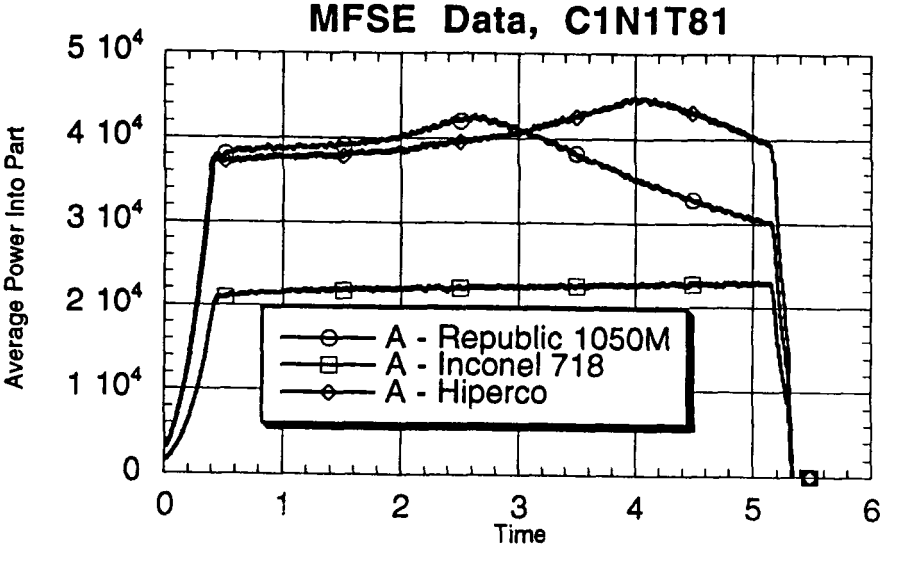

Figure 2. Variation of a selected process signal with material. Republic 1050M is a ferromagnetic carbon steel, IN 718 is a paramagnetic material, and Hiperco is a ferromagnetic material with a high Curie temperature.

importance of having multiple characteristic process signals that change as the process progresses and which vary across the process parameter space is that an unambiguous correlation does not exist between a single signal and the depth of hardening. Thus, the use of neural network techniques to find subtle, nonlinear correlations between signal features and the depth of hardening is critical to the success of this project. The ability to relate characteristic process signals to metallurgical changes occurring in the parts using the computational model enabled rational selection of signals and signal features for establishing closed-loop control. Physical models of the process decrease the training requirements of the neural network by indicating the most critical parameters of the process.

Saginaw Experiments

Second year activities for the process characterization task included factor space experiments designed to identify the effects of heat-to-heat material variations and geometry effects on the characteristic process signals. The task provided support for controller development as a number of prototype control algorithms were evaluated. Additionally, data collection and evaluation experiments in Delphi Saginaw's induction laboratory, development of alternative methods to measure coil current at the coil, and support of modeling experiments were part of the year's accomplishments.

Experiments were conducted in Delphi Saginaw's induction lab to determine if the signal processing algorithms would work equally well on a completely different power supply, and to examine the characteristic process signals that result from scanning. To evaluate power supply differences, the coil and specimens used for experimentation at Sandia were used at Saginaw with a power supply from their induction lab. The data acquisition system was identical to the system at Sandia and was purchased by Saginaw for their use with this project. The signal processing was done in software. Data was collected from single shot runs on both 4" long round bars and spline end bars of the same heat of steel.

The voltage and current waveforms from the Saginaw power supply were damped sinusoids rather than the chopped waveforms observed with the power supply in the Sandia laboratory. However, characteristic signals such as power into the part and energy into the part had identical features and similar magnitudes. Collection of data from a relatively small number of samples, approximately 20, allowed training of a neural net that predicted case depth to +/- 0.1 mm for the one heat of material used in these experiments. This was demonstrated for the Delphi Saginaw process engineers by running the process, then processing the data and predicting the case depth. The specimens were then sectioned and the case depth measured. The predictions were consistently found to be accurate.

Scanning processes were also characterized in the Delphi Saginaw induction lab. The machine was set up with a standard scanning coil and operating parameters for a common production axle. Both round bars and fully machined axle bars were scanned. The voltage and current signals were acquired in a manner identical to the single shot experiments and the data was processed by the Sandia-proprietary software for signal processing.

One of the characteristic process signals, total resistance, is shown in Figure 3 for a round bar scan-hardened using nominal production settings for the induction machine. Since the scanning rate and

heating parameters were changed by the machine logic over the scanning cycle it is not possible to directly relate signal characteristic variations to variations in material properties in the part, but the changes observed appear to be similar to the changes that occur in single shot processes. The same signal from an axle bar showed dips in the signal associated with reduced diameters and snap ring grooves, i.e. changes which reflect changes in coupling between the part and the induction coil.

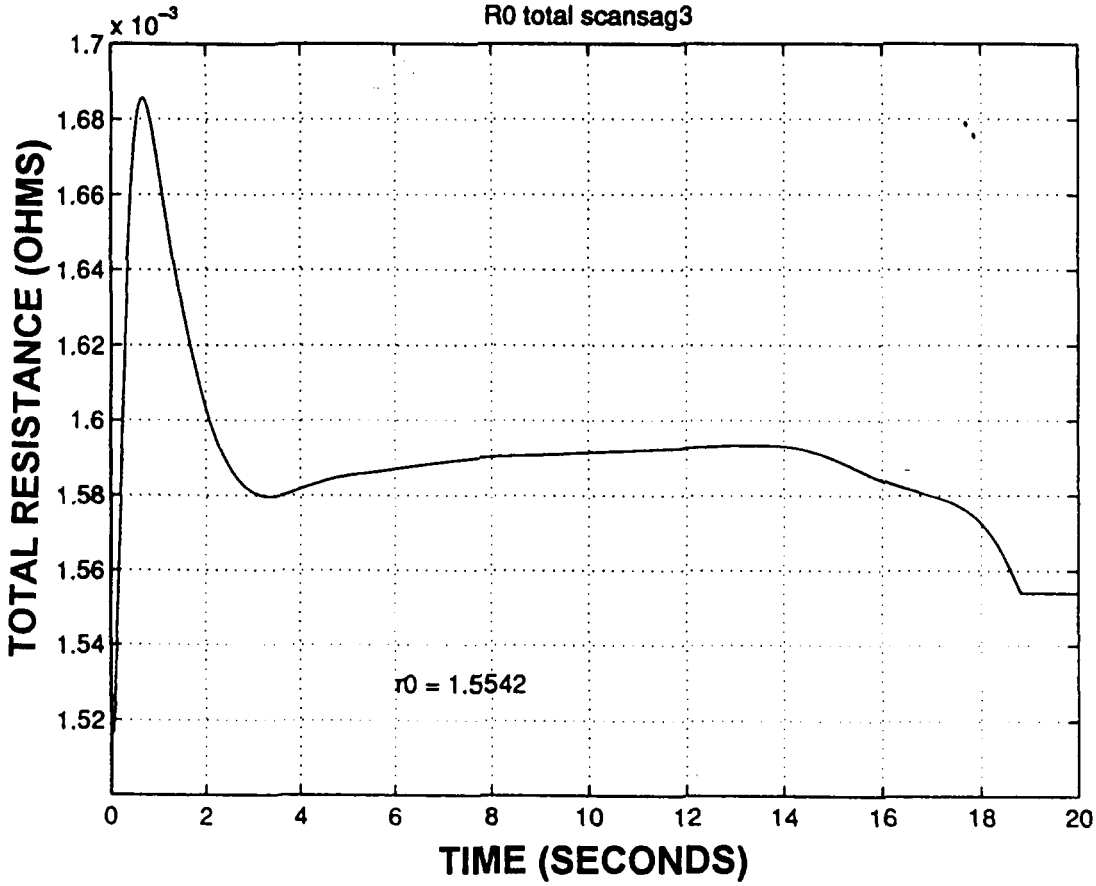

Figure 3. Total resistance in the induction coil derived from voltage and current measurements at the coil leads.

The characteristic signals from scanning processes revealed that different and more complex control algorithms would be necessary to control scanning processes. Controls may have to encompass the heating process as well as the scanning drive controls in order to enable delivery of a specific amount of energy to the coupled volume of material and allow optimization of the induction process and component properties. This kind of control algorithm will enable much more precise control of the heat treatment process and optimization of the processing and properties of induction hardened components.

Process Signal Measurement

The experiments in Delphi Saginaw's induction laboratory emphasized the need to have alternative current measuring devices available, if possible. It was found that installation of a Rogowski coil for current measurement at the induction coil is intrusive and requires, in some cases, undesirable redesign of the coil and machine. This is a concern Delphi Saginaw personnel expressed several times in the project.

Pulsed Power Physics expertise was applied to design and fabricate current sensors called B-dot sensors for current measurement in the high electromagnetic field environment at the coil. These sensors monitor changes in the magnetic field strength by producing a proportional voltage. However, their output is sensitive to nearby structures which distort or change the magnetic field. Shielded B-dot probes were fabricated with non-magnetic materials to allow the use of these probes in a variety of environments. B-dot probes were evaluated in a number locations around the coil and current data was collected simultaneously with the Rogowski coil.

Current signals from B-dot probes were similar to the current signals from the Rogowski coil in shape. Magnitude was calibrated by using the Rogowski coil signal as a gage. Thus, current signals from B-dot probes were suitable for use by the signal processing algorithms which generate the characteristic process signals. However, when the Rogowski coil and B-dot signals were collected simultaneously and then overlaid, there was always some offset between the two as shown in Figure 4. This apparently small difference in signals resulted in significant differences in the magnitudes of the characteristic process signals such as energy and power into the part. Since the signal processing algorithms were validated using data from the Rogowski coil and agreed closely with the results of the calorimetry, it was concluded that the B-dot probes were less accurate for use than the Rogowski coil.

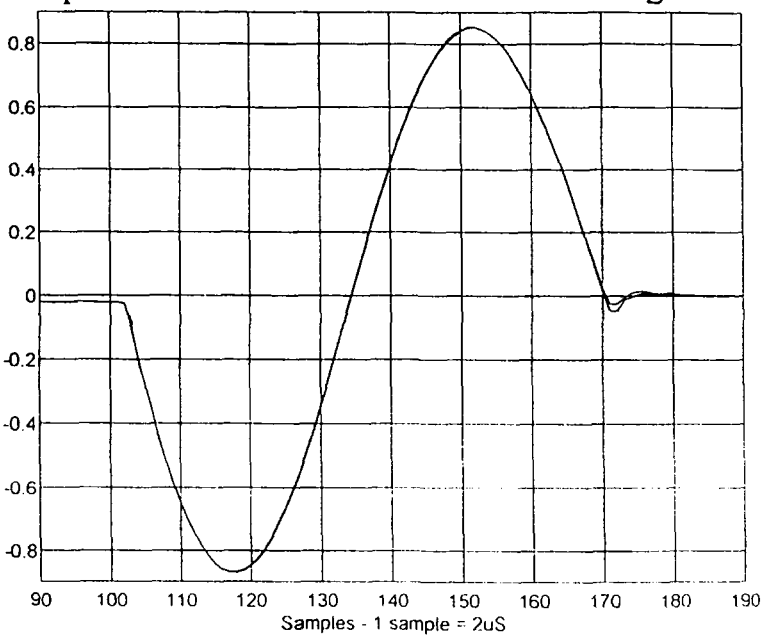

Figure 4. Comparison of current measurements made with the B-dot probe and the Rogowski probe. The Rogowski coil measures a slightly larger negative current peak at the second zero crossing.

Induction machines also have an internal current sensor used by the machine to regulate the power delivered to the part being heated. This internal current sensor was also evaluated for use as the current monitor device for the Sandia control algorithm. In the Sandia lab machine, this sensor was located prior to the output transformer. The sensor produced similar waveforms which were phase-shifted in a non-linear way from the signal collected with the Rogowski coil. In this sense it provided a signal similar to the signals from the B-dot probes. Although the signals from the B-dot probes and the internal sensor could be used for current measurement and to generate characteristic process signals for controller purposes, using these devices essentially decouples the control algorithm from the process fundamentals. Ultimately, it was concluded that this process signal was less desirable for process control purposes.

Factor Space Experiments

During the course of the second year, over two hundred steel specimens were hardened with support from the Process Characterization task to generate the data necessary for the Controller Development task. Over half of these specimens were fabricated from Inland Steel heats provided by Delphi Saginaw and stockpiled for this purpose. The remainder were specimens provided by Delphi Saginaw originally from a Republic Steel heat. Experiments were initially conducted using software data processing algorithms in order to determine what data were needed to be extracted from the characteristic signals for control purposes. Later experiments were conducted with the data processing algorithms embedded on a circuit board which extracted the required information and provided a feedback signal for processs control. The circuit board hardware significantly simplified data acquisition and analysis by preprocessing the signals and thereby reducing the routine computations. Factor space experiments to characterize heat-to-heat variations in input materials and the effects of geometrical differences were delayed until the circuit board hardware was fully developed.

The materials factor space was conducted to characterize the differences between heats of steel from one supplier. Delphi Saginaw provided bars from 36 heats of 1050M steel from Inland Steel Bar Company as shown in Table I. Delphi characterized these heats with respect to chemistry and hardenability as shown in the table and provided copies of the steel mill certification report as well as their own characterization report, the "T" report.

A fractional factorial experiment was conducted across the standard range of power and time settings determined last year, and across the range of heat-to-heat variations. The heats were divided into three ranges of carbon content and ideal diameter, D_I, the hardenability factor used by Delphi Saginaw to specify their materials. The specified carbon content for the steel is 0.46-0.54% carbon by weight, so the heats were assigned a value of "-" for carbon contents of 0.46-0.49%, "0" for carbon contents of 0.49-0.51, and "+" for carbon contents of 0.51-0.54%. The ideal diameter range represented by these heats was 1.14-1.64 inches, so the heats were assigned a value of "-" for D_I in the range of 1.14-1.28, "0" for D_I in the range of 1.29-1.48, and "+" for D_I in the range of 1.49-1.64. From this matrix of heat-to-heat variables, it was desired to select heats to be representative of the largest differences

Table I. Description of 36 heats of 1050M steel provided by Delphi Saginaw for factor-of-space experiments.

INDUCTION HARDENING MATERIALS HARDNESS COMPARISON				
				T Report
			T Report	Carbon
T Report #	Material	Heat #	Chemistry DI	Content
T97579	Inland 1050M	98343	1.37	0.49
T97934	Inland 1050M	98854	1.35	0.50
T97947	Inland 1050M	98626	1.14 *min	0.477
T97967	Inland 1050M	98845	1.49	0.48
T97968	Inland 1050M	98846	1.40	0.475
T97969	Inland 1050M	98847	1.57	0.47
T98146	Inland 1050M	98927	1.42	0.465 *min
T98147	Inland 1050M	98859	1.38	0.473
T98148	Inland 1050M	98860	1.41	0.49
T98150	Inland 1050M	98856	1.33	0.48
T98151	Inland 1050M	98858	1.36	0.49
T98363	Inland 1050M	99483	1.43	0.465 *min
T98366	Inland 1050M	99476	1.39	0.463 *min
T98367	Inland 1050M	99477	1.29	0.463 *min
T98385	Inland 1050M	99486	1.40	0.463 *min
T98805	Inland 1050M	90082	1.44	0.49
T98806	Inland 1050M	99958	1.53	0.52
T98810	Inland 1050M	47881	1.52	0.52
T98812	Inland 1050M	99971	1.52	0.49
T98859	Inland 1050M	99485	1.37	0.52
T98918	Inland 1050M	90099	1.62	0.51
T98919	Inland 1050M	90104	1.59	0.51
T98920	Inland 1050M	90105	1.62	0.52
T99130	Inland 1050M	90474	1.57	0.54 *max
T99266	Inland 1050M	90674	1.58	0.51
T99267	Inland 1050M	90673	1.50	0.48
T99352	Inland 1050M	90860	1.64 *max	0.54 *max
T99479	Inland 1050M	91045	1.33	0.495
T99556	Inland 1050M	91159	1.55	0.505
T99557	Inland 1050M	91160	1.52	0.50
T99558	Inland 1050M	90890	1.48	0.483
T99580	Inland 1050M	90858	1.31	0.47
T00054	Inland 1050M	91520	1.46	0.495
T00055	Inland 1050M	91167	1.61	0.51
T00179	Inland 1050M	91981	1.36	0.485
T00180	Inland 1050M	91814	1.37	0.475

between heats. Five heats were selected to be representative of the corners of the matrix, plus a centerpoint, i.e. a "++" heat, T99130 (high D_I, high carbon), a "+-" heat, T98812 (high D_I, low carbon), a "-+" heat, T98859, a "--" heat, T97947, and a "00" heat, T97934. It should be noted that heat T98859 was actually a "0+" per the above matrix, but it was the closest heat to a "-+" combination in the heats collected.

Analysis of the results of the factor space experiment revealed no consistent variations in response with carbon content or ideal diameter. As shown in Figure 5, there was not much difference nor was there consistent variation in case depth from heat-to-heat at any of the power/time settings used in the factor space. As shown in Figure 6, the maximum energy into the part varied significantly with power and time settings across the factor space, but for any given power/time point in the factor space there was virtually no variation in energy into the workpiece. This points out a significant advantage of using neural networks in this project. Neural networks are able to account for subtle, non-linear differences in the heats of material. As shown in a later section of this report, using D_I and weight percent carbon as inputs to the neural network, and monitoring the characteristic signals, a neural network was trained with an accuracy of +/- 0.1 mm across the range of heat-to-heat variations represented by the samples collected by Delphi Saginaw.

In order to evaluate the validity of the approach used to encompass variations in component geometry, two fractional-factorial experiments were conducted at the power and time settings determined previously. The first experiment used 4 inch long right circular cylinder specimens with reduced diameters which ranged from 0.8 inches to 0.9 inches. The 0.9 inch diameter is representative of the reduced diameter section of the target application axle bar. Case depth varied consistently with diameter, power and time, as expected. The most important finding was that the characteristic process signals had similar features but different absolute values as shown in Figures 7a and 7b. Changing the diameter changed the coupling between the part and the coil resulting in less energy into the workpiece and reduced resistance as measured by R0, but the features of the signals were identical. Thus, the control algorithm is suitable for use across a broad range of reduced diameters.

The second geometry factor space compared the resulting characteristic signals from standard four inch long round bars versus splined bars cut from the ends of actual axle shafts. These specimens are shown in Figure 8. The purpose of this experiment was to determine if the signal processing and control algorithms were suitable for use with more complex geometries associated with actual parts containing splines, reduced diameters, and snap ring grooves. As with the reduced diameter bars, the characteristic signals had similar features but different absolute values as shown in Figures 9a and 9b. Thus, it was determined that the signal processing and control algorithms were suitable for use across the full range of geometries targeted for this project.

The knowledge gained in the materials and geometry factor space experiments, as well as the experiments conducted in Delphi-Saginaw's induction laboratory, provided critical information for the selection of a specific application for implementation of our process control technology on the factory floor. After careful consideration, Delphi Saginaw and Sandia chose to focus the third year effort on control and process optimization for the Saturn Intermediate Shaft. The shaft is larger than the axle bars used in the experiments at Sandia's facility, but the process and induction machine were similar to the process and machine at Sandia. The manufacturing schedule of the Saturn Intermediate Shaft allows for real-time experimentation since it is not a three-shift operation.

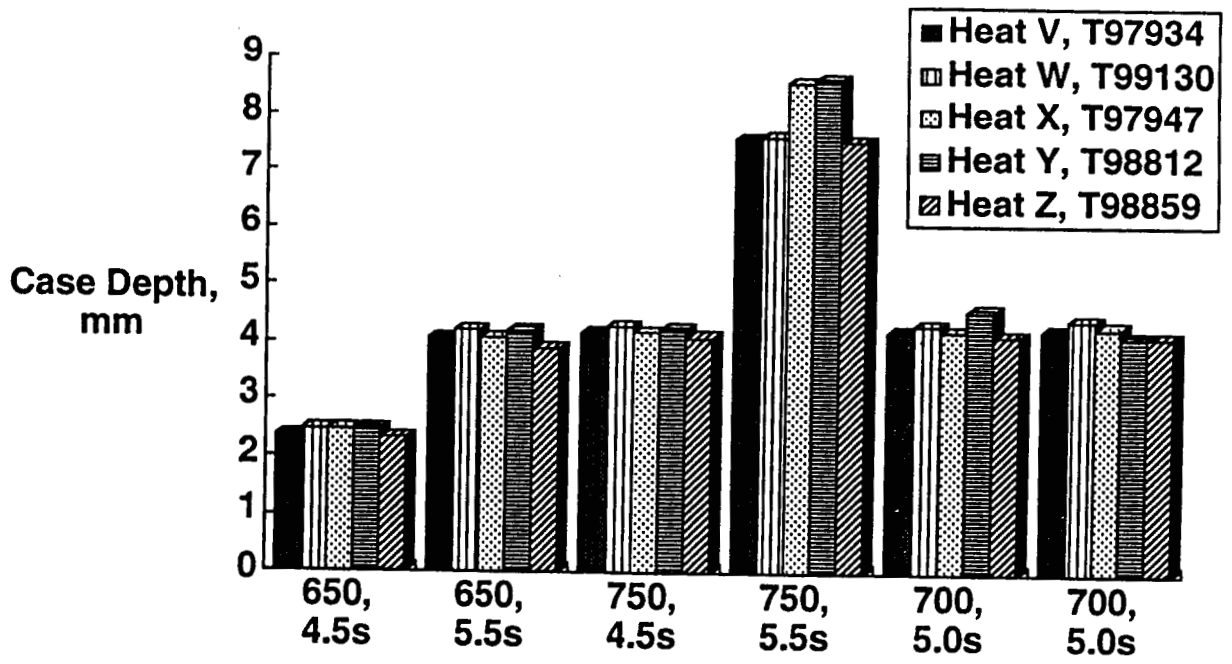

Figure 5. HRC 50 case depth variation from heat-to-heat with fixed control setting on the induction power supply.

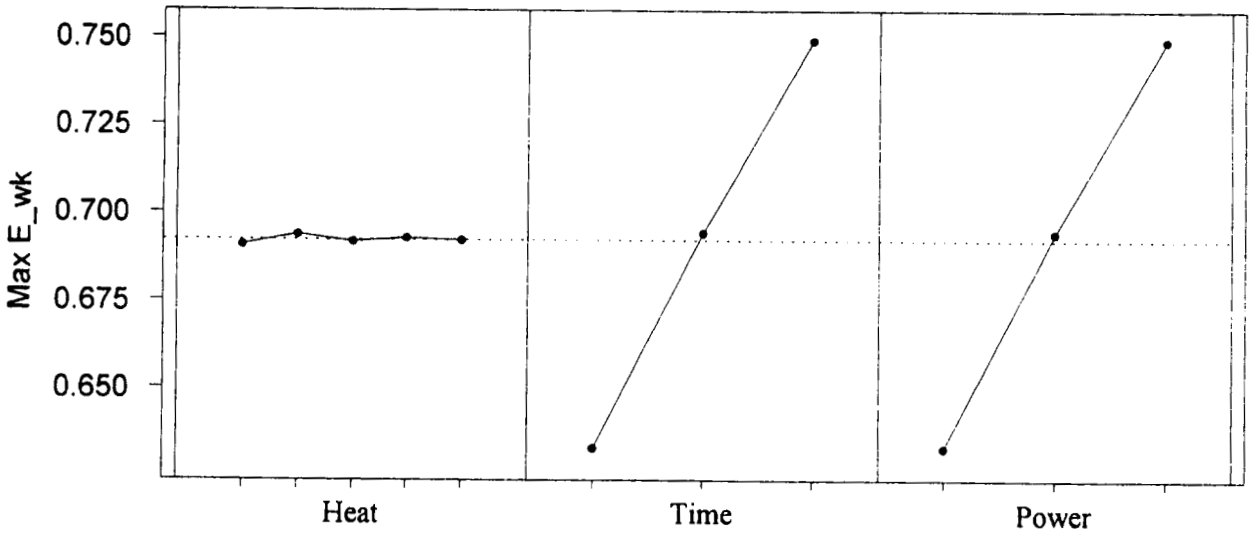

Figure 6. Comparison of the maximum energy to the part with variations power and heating duration settings on the induction power supply.

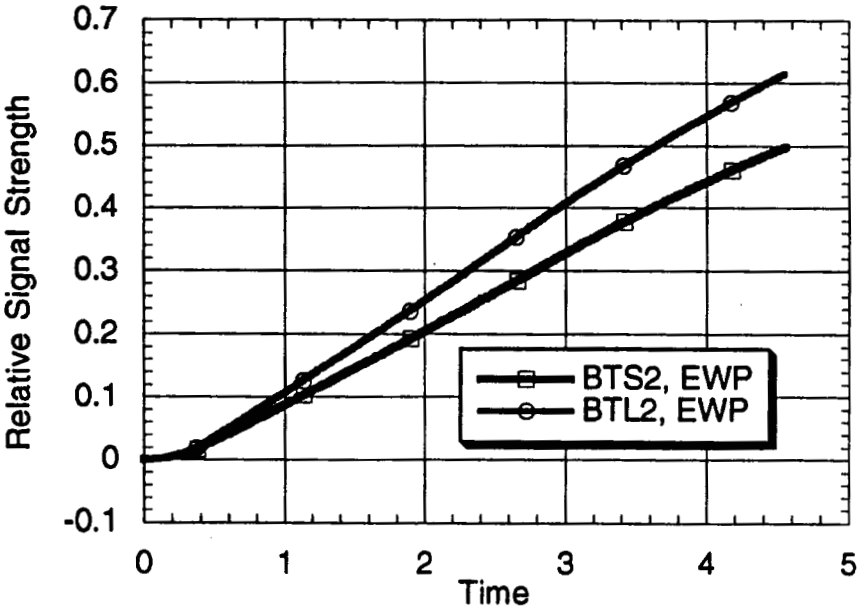

Figure 7a. Influence of part diameter on the energy to the workpiece. BTL2 had a diameter of 0.9 inches and BTS2 had a diameter of 0.8 inches.

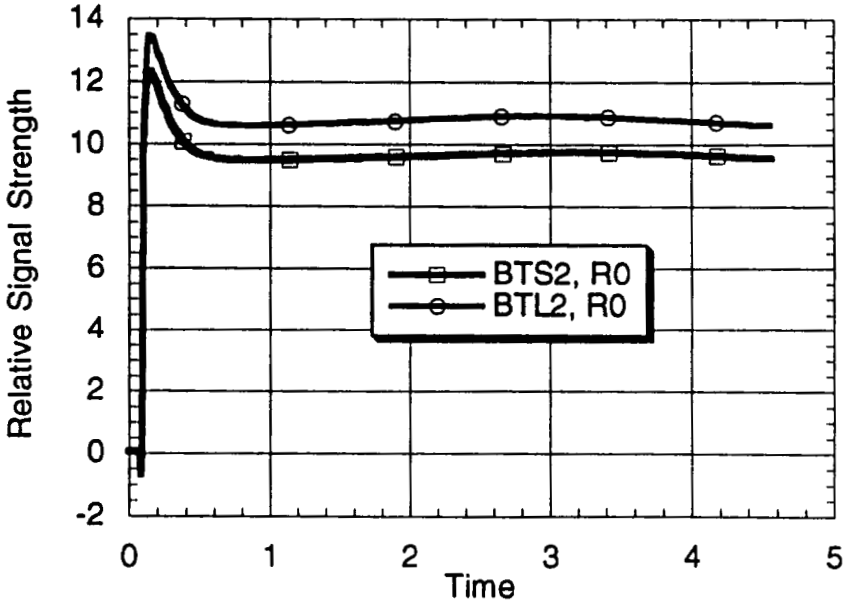

Figure 7b. Reduction in normalized total resistance resulting from a reduction in the part diameter. BTL2 had a diameter of 0.9 inches and BTS2 had a diameter of 0.8 inches.

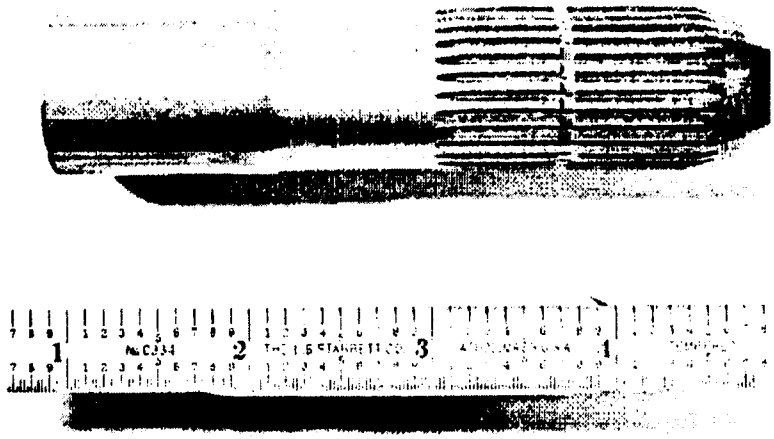

Figure 8. Splined rod geometry used for complex geometry tests

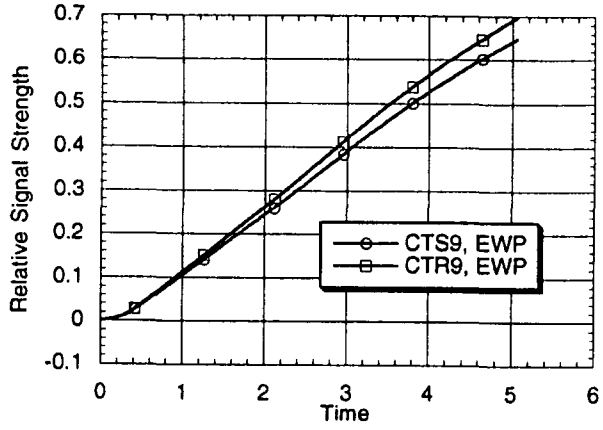

Figure 9a. Energy to the workpiece for a splined shaft. CTS9 had splines and CTR9 had no splines

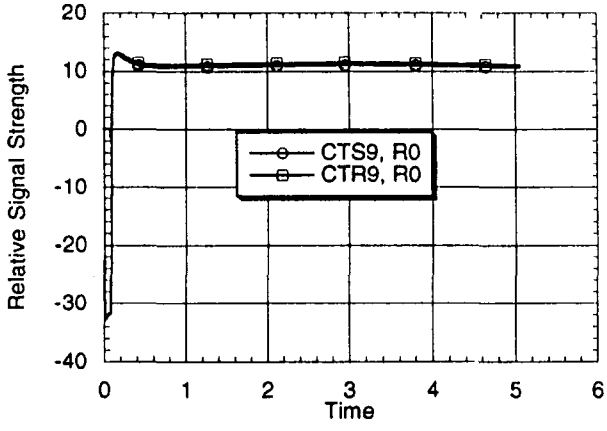

Figure 9b. Total resistance for a splined shaft workpiece. CTS9 had splines and CTR9 had no splines

MATERIAL TASK

The basic goal of the Materials Characterization Task is to identify and characterize the materials properties which are critical in determining the response of the material to the induction hardening process. In particular, the intent is to understand the relationships between heat-to-heat variability and variability in the hardening response so that control algorithms can be designed to compensate for the differences. The variation from heat-to-heat can be divided into variation in the response of the heat to a given thermal cycle (i.e. what transformations occur and at what rate for a given time-temperature path?) and variation in the thermal response of the material to a given energy input (i.e. what thermal cycle results from a fixed energy input?). The variation of hardening response for specific thermal cycles has been the focus of the second year of the project, although experiments to assess the response to input energy have also been designed.

Approach

During the second year of the project, three primary approaches have been taken. These are: (1) Expansion of the hardenability/quench severity analysis developed during the first project year; (2) Collection of 1050M heats and development of a database for chemistry, D_I, Jominy hardenability, microstructure, and cleanliness; (3) Development of experimental and analytical methodologies for determining the on-heating transformation kinetics. Each of these approaches are discussed below in terms of their relationship to the project goals and the results to date.

Hardenability/Quench Severity Analysis

The basis of the of the hardenability/quench severity analysis was described in the first year report and is discussed in detail in a paper by Knorovsky et al. [1995]. There are two major aspects to this work: (1) An evaluation of the effect of nonisothermal temperature profiles (*e.g.* surface heated) on cooling rates during quenching, and (2) Development of an analysis procedure and estimates of case depth variation due to variation in ideal diameter (D_I) and quench factor (H).

The evaluation of the effect of nonisothermal temperature profiles was conducted by finite element modeling and comparing the cooling rates at various depths in 1 inch diameter bars. Comparisons were made between bars which were either uniformly heated throughout, or had temperature profiles similar to those in induction heated shafts. In essence, the results of this work showed that the cooling rates for the given bar size and quenching conditions were not strongly affected by the initial temperature profile. As a result, it is acceptable to use quantitative hardenability theory (which was developed for uniformly heated material) to assess the influence of variations in D_I and H.

The results of the analysis of case depth variation as a function of ideal diameter and quench factor are summarized in Figure 10. The figure shows case depth (as a fraction of the diameter) for a 1 inch diameter bar isothermally heated to austenite. The case depth in Figure 1 is calculated from quantitative hardenability theory. The figure also shows the D_I range given by the GM specification. As shown, two hardening regimes can be identified; that in which the hardened depth is limited by the hardenability of the material, and that in which the hardened depth is limited by the depth to which the part is austenitized. For the 1050M steel used at Saginaw and in the experimental program at Sandia, the hardenability (D_I) and quench factor (H) are sufficient to insure that the hardening operation is in the depth-of-heating limited range. Further evidence of this conclusion is that samples in the various factor space experiments at Sandia could be fully hardened to the center of the bar, thereby demonstrating that the hardenability and spray quench are sufficient.

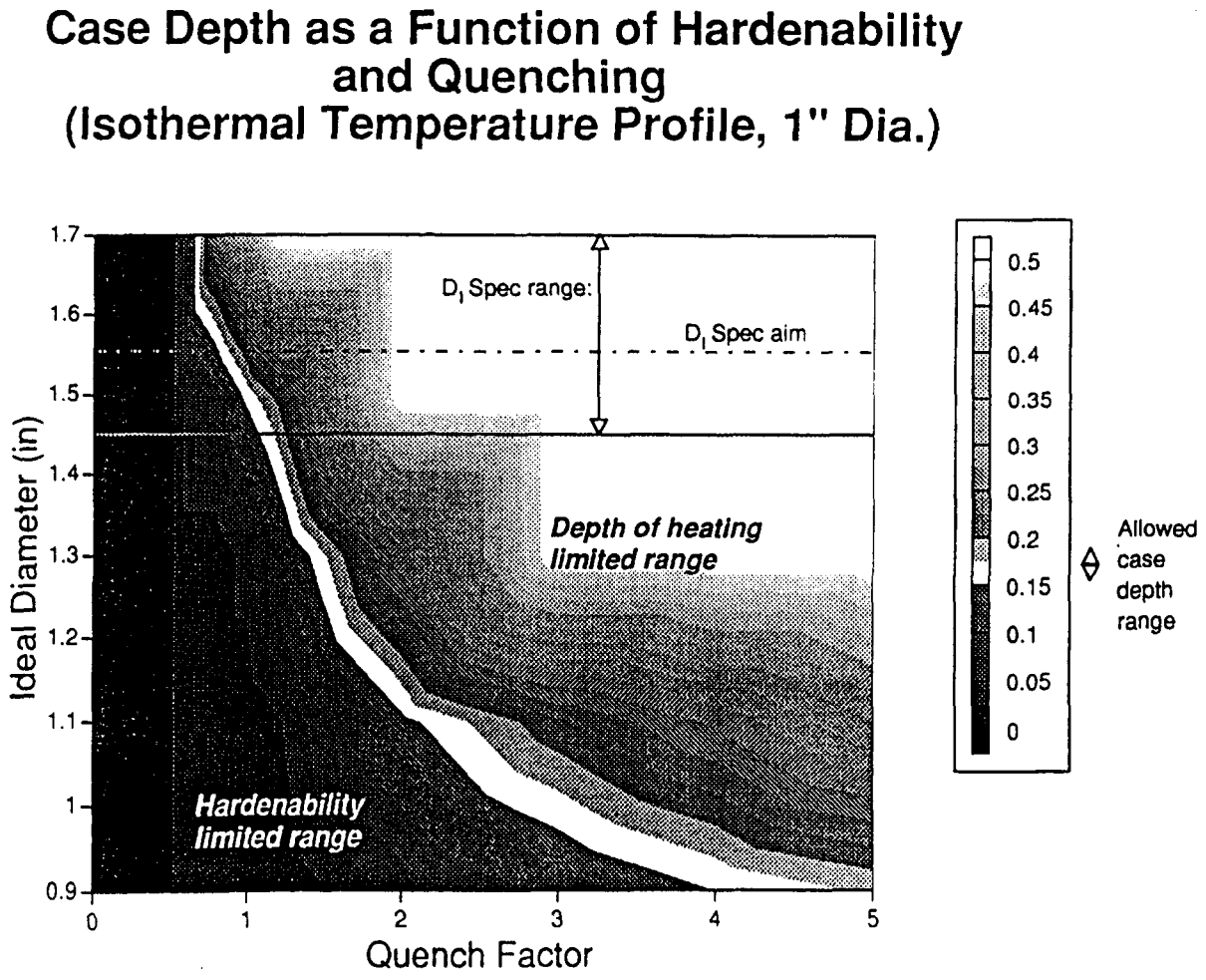

Figure 10. Case depth as a function of hardenability and quench severity for an isothermally austenitized 25.4 mm diameter bar. The current Saginaw Specification aim and range for D_I are indicated on the figure.

There are several important implications to the observation that most induction hardening processes are operating in the depth of heating limited range. The first of these implications is that process control schemes based on consideration of the energy into the part, such as the neural network approach being used at Sandia, are physically appropriate. Secondly, from a materials perspective, the hardening process is controlled by the on-heating transformation to austenite rather than the on-quenching transformation to martensite. Finally, since the formation of austenite is mechanistically different than the formation of martensite, *traditional hardenability parameters such as D_I or Jominy end quench testing may not adequately describe heat-to-heat variations in induction hardening*. A more suitable measure is likely to be the austenite formation kinetics at induction heating rates. Means for comparing steel heats in terms of the variation in austenite transformation kinetics are under development, and are discussed more fully below.

Materials Database

Through agreement with Saginaw, approximately 40 heats of 1050M bar stock were stockpiled during the year. These heats have been evaluated at both Saginaw and Sandia using a variety of techniques, and have also been used in a number of induction hardening factor space experiments. The intent of this effort is to establish a materials database from which realistic heat-to-heat variations can be assessed. At Saginaw, the following were determined for each of the heats: heat chemistry (as determined by both the steel producer and the Saginaw chemical analysis laboratory), Jominy end quench hardenability, macrostructure and grain size, and inclusion rating. Figure 11 shows an example of these determinations, and represents the Jominy response for twenty three of the stockpiled heats. From the results of this work, extremes in Jominy hardenability were selected for comparison in terms of induction hardening response. In general the hardening response of the these heats, though not dramatically different, did not follow the trends that might be expected from the Jominy behavior. Following the discussion in the previous section, this observation is not unreasonable since the Jominy test is a traditional measure of hardenability (*i.e.* is indicative of the on-cooling rather than on-heating behavior of the steel). Laboratory induction hardening tests of steel heats with extremes of D_I and carbon content, which are again primarily measures of on-cooling response, yielded results similar to that for the Jominy comparison.

At Sandia, the magnetic properties of the heats as a function of temperature have been evaluated and the austenitization kinetics are being determined. Discussion of the results of the magnetic measurements is presented in the Computational Modeling section of this report. The determination of austenitization kinetics and its relationship to control philosophies is discussed in the following section.

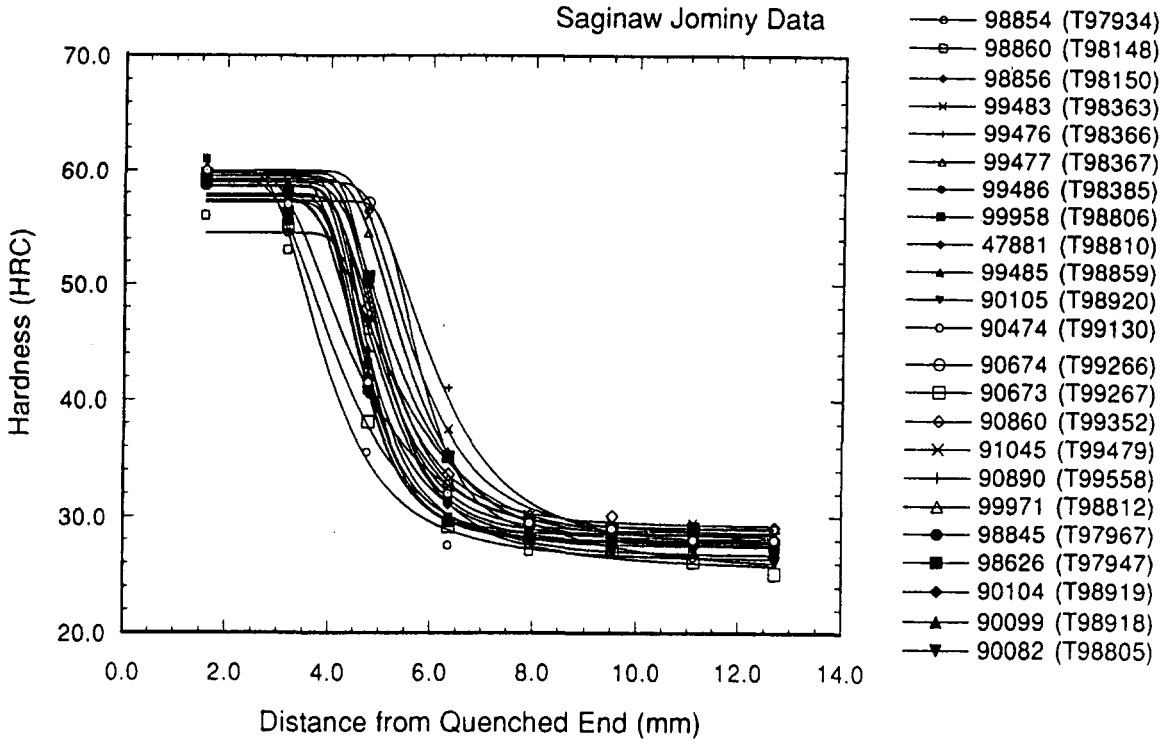

Figure 11. Jominy results for twenty three stockpiled 1050M steel heats. The curve fits shown are based on a four parameter fit of the form HRC = A-[Bexp(CJ^D)].

Austenitization Kinetics

Figure 12a shows the results of thermocouple measurements of induction heated 25 mm diameter cylinders hardened to a depth of approximately 5 mm. Measurements are shown for the part surface, 1/3 radius, 2/3 radius, and center. For typical shaft applications, the hardened depth is also on the order of 4-5 mm, so the 2/3 radius thermal cycle is indicative of the thermal cycle near the root of the case. As shown, the time above the first temperature at which austenite becomes stable (A_{e1}) is comparatively short and is on the order of approximately 2 seconds. In addition, the shape of the thermal cycle above A_{e1} is approximately parabolic. Clearly, the austenite formation kinetics must be defined for this type of thermal cycle.

Figure 12b shows an actual thermal cycle (run in a weld thermal cycle simulator) for the austenite transformation kinetics study. In this thermal cycle, a two second linear ramp to 710°C (A_{e1}) is followed by a two second parabolic cycle to a peak temperature of 830°C. As the temperature reaches A_{e1} on the cooling portion of the parabola, a helium spray quench is applied to insure that all the austenite which had formed is transformed to martensite. The fraction martensite and hardness can then be measured. Determination of the transformation kinetics in

this manner has two principal advantages over other approaches. First, the simulation experiments allow for direct comparison of the heats following thermal cycles which are very similar to induction thermal cycles. Secondly, since the relationship between time and temperature is fixed by the parabolic shape, kinetic parameters can be determined in a comparatively small number of experiments. For this work, the approach described by Ashby and Easterling [1984] is being explored. The approach considers the transformation in hypoeutectoid steels to proceed initially by transformation of the pearlite, followed by transformation of the proeutectoid ferrite. Both processes are controlled by carbon diffusion. It is expected that the simulation experiments and analysis will yield a materials "characteristic" which will be applicable to control algorithms. In addition, by selecting peak temperatures between A_{e1} and A_{e3}, heat-to-heat variations in the positions of the phase boundaries can be assessed.

Initial results using the parabolic thermal cycles have shown differences between heats. For example, Figure 13 compares the hardness of two 1050M steel heats following thermal cycles which consisted of a two second linear ramp to 710°C followed by a three second parabolic cycle above that temperature and a helium quench. The data is shown in terms of hardness as a function of peak temperature for the parabolic cycle. At high temperatures where austenitization is complete, the two steels show essentially the same hardness. However, for peak temperatures near and below the upper critical temperature (770 and 740°C) the steels display significantly different hardness. These two heats have previously been shown to have a factor of two difference in prior austenite grain size, with the Bethlehem heat being finer. The results of Figure 4 are therefore consistent with the microstructural observations and the transformation mechanism described by Ashby and Easterling [1984], since the finer microstructure can be expected to transform more rapidly.

If it is assumed that the fitted curves of Figure 13 are reasonable representations of the hardness as a function of peak temperature, it is possible to develop a first order estimate of the difference in hardening depth expected for these two steels. To achieve a hardness of 50 HRC, the two steels require slightly different peak temperatures (approximately 748 and 756°C for the three second parabola). From Figure 12a, a curve of depth versus peak temperature can be constructed and the derivative of this curve at a peak temperature of 750°C is roughly 0.03 mm/°C. Thus, for the 8°C difference in peak temperature, the expected variation in hardened depth is on the order 0.24 mm. Clearly this estimate is only approximate and requires substantial refinement. However, the estimate demonstrates that variation in the on-heating transformation behavior can result in significant variation in the hardening response.

Following refinement of the kinetic measurement methods and analysis, the stockpiled 1050M heats will be compared. In addition, Saginaw has also supplied machined samples of a number of other steels which are induction hardened. These materials will also be evaluated in terms of their on-heating transformation kinetics.

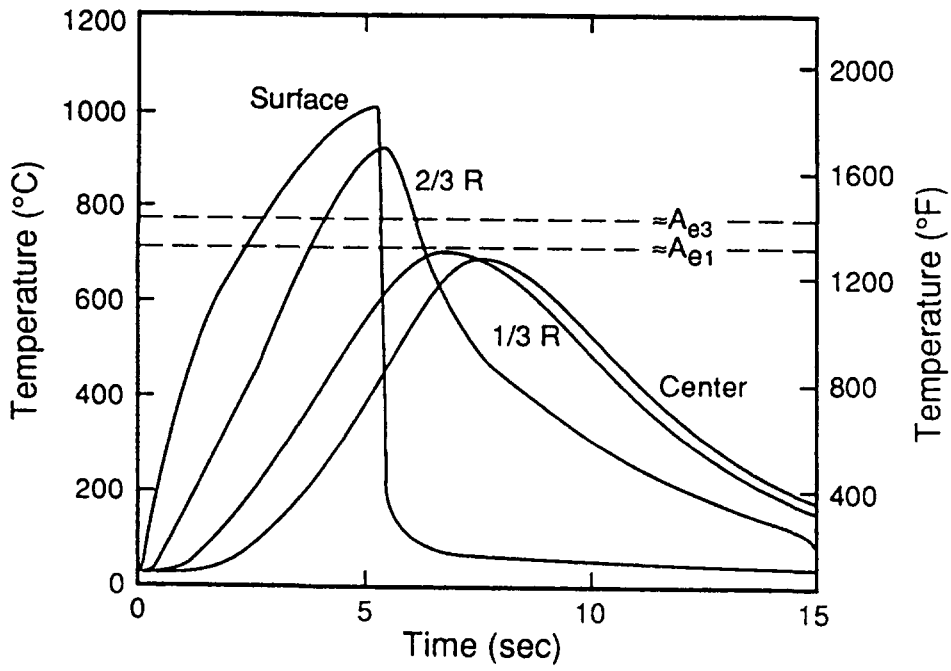

Figure 12a. Results of thermocouple measurements for a 25 mm diameter cylindrical bar induction hardened to approximately 5 mm case depth.

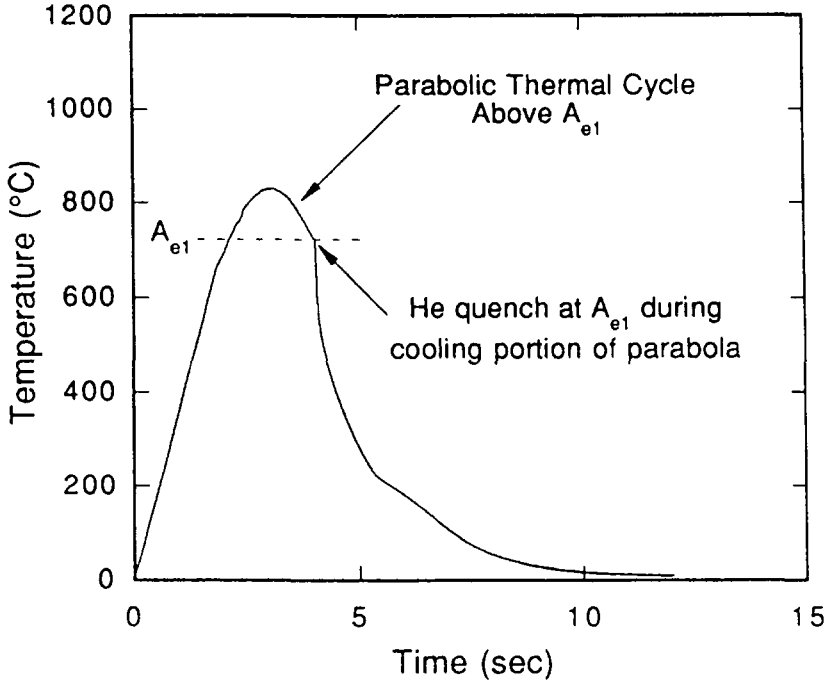

Figure 12b. Typical thermal cycle used for evaluation of austenitization kinetics.

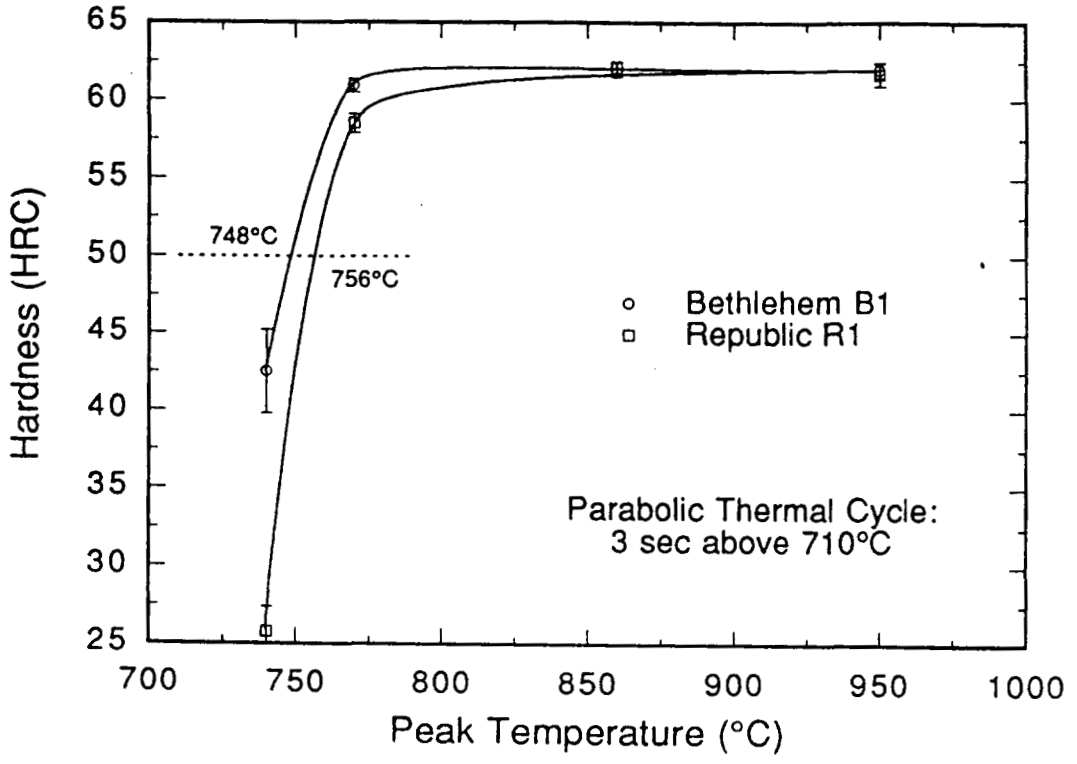

Figure 13. Comparison of hardness for two 1050M heats following thermal cycles consisting of a two second linear ramp to 710°C followed by a 3 second parabolic cycle above that temperature and a helium quench.

COMPUTATIONAL MODELING TASK

The computational modeling task of the induction heating CRADA with General Motors has four primary objectives:

- *Develop a fundamental understanding of the induction heating process*
- *Aid in the interpretation of experimental results*
- *Assist in the development of controls*
- *Determine the significance of material properties.*

These tasks are intended to maximize the likelihood that we produce a science-based control system that accurately controls the depth of hardening in automotive parts. To compliment the control development efforts, the modeling task is also committed to developing a computer model that can predict temperature profiles in parts during the induction heating process.

Approach

During the second year of this project, three major activities were undertaken in the Computational Modeling Task. These activities are as follows: (1) Confirm power estimates derived from electrical signals, (2) Study electromagnetic variations in axle materials and the impact of these variations on the induction heating process, (3) develop a 3-D model to predict temperature profiles in inductively heated parts and verify the model with experimental results. The Computational Modeling Task activities are described more fully in the following paragraphs.

Validation of Power Estimates

One of the unique contributions of this program is a system model that allows us to calculate the power and energy that is delivered to the part and the coil. These calculations are based upon the electrical signals from the coil, and the calculation routines are described in the first annual report of this CRADA [Adkins et al, 1994]

A calorimeter system was developed that allows us to verify the results of the power predictions. The energy distribution in the part/coil system that was measured with the calorimeter and predicted with the electrical signature analysis is shown in Figure 14. Calorimeter measurements on water-cooled part showed that 73 kJ of energy went into the part and about 10 kJ went into the water cooling the coil. It was estimated that about 10 kJ was conducted up the bus to the coil and roughly 6 kJ went into heating the coil. Based on the electrical signature, 75 kJ went into the part and 98 kJ went into the coil/part system. The part energy predictions matched well with the calorimeter measurements, and the energy prediction into the entire system was reasonable once the estimates for the stored and conducted energy were included.

The water-cooled part had a rapid response time, and because it was water-cooled, it was possible to run the system to a steady state condition. Under steady conditions, the measured power to the part was 18.8 kW, and the power based on the electrical signature was 19.3 kW.

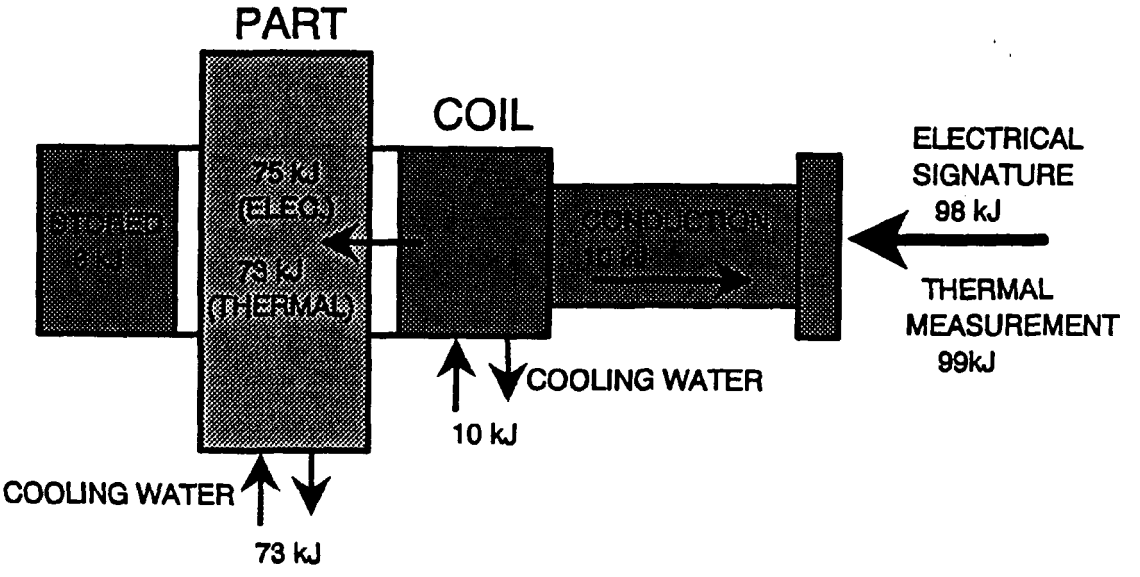

Figure 14. Energy distribution in induction heating system measured through calorimetry and electrical signal data reduction. Stored energy and conduction away form the coil are estimated.

The calorimetry work showed that the electrical signature analysis could predict the power to the part to within 3%.

Electromagnetic Property Variations in Materials

In the first year of this CRADA, a one-dimensional computer model was developed that predicts temperature profiles in cylindrical axle stubs in a long induction coil. Along with the temperature predictions, the model also illustrates the impact that property changes have on the power that is transferred from the induction coil to the part. As the surface temperature of the part exceeds the Curie temperature, the total power that is transferred to the part declines. This phenomena is also observed in the power signal that is derived from the electrical measurements on the coil.

The importance of the Curie temperature on the heating profile in the part becomes apparent when a comparison is made between the influence of various properties, such as Curie temperature, hysteresis losses and electrical resistance. Figure 15 shows the predicted temperature profile at the end of the heating cycle in a 23.8-mm diameter 1050 steel stub. At the end of the 5-

second heating cycle, the core of the stub was above 600°C, and the 780°C Curie temperature was exceeded at a depth of 5 mm for all four cases. Figure 15 shows that a 10% increase in hysteresis losses has virtually no effect on the heating profile, and a 10% increase in the electrical resistance only slightly lowers the final temperatures. Increasing the Curie temperature by 20°C, however, causes the surface temperature to increase by 40°C when compared to the base case. In fact, the temperature profile throughout the part increases with the higher Curie temperature which indicates that the part has absorbed more energy.

Since the Curie temperature does not appear in material specifications, variations among steel suppliers and material lots from the same producer could influence the induction hardening of parts. The magnetic properties of the production steels generally are not known in detail. A system to measure the magnetic properties of steel samples as both a function of temperature and frequency was constructed at Sandia. The hysteresis measurement system is shown schematically in Figure 16. The material in question is cut into thin washers that are laminated together to form the core of a transformer. A current through the primary winding of the transformer creates a magnetic field around the core, and the resulting magnetic flux in the material is detected with the secondary coil. The samples are placed in an oven to control the temperature while the magnetic hysteresis properties are measured.

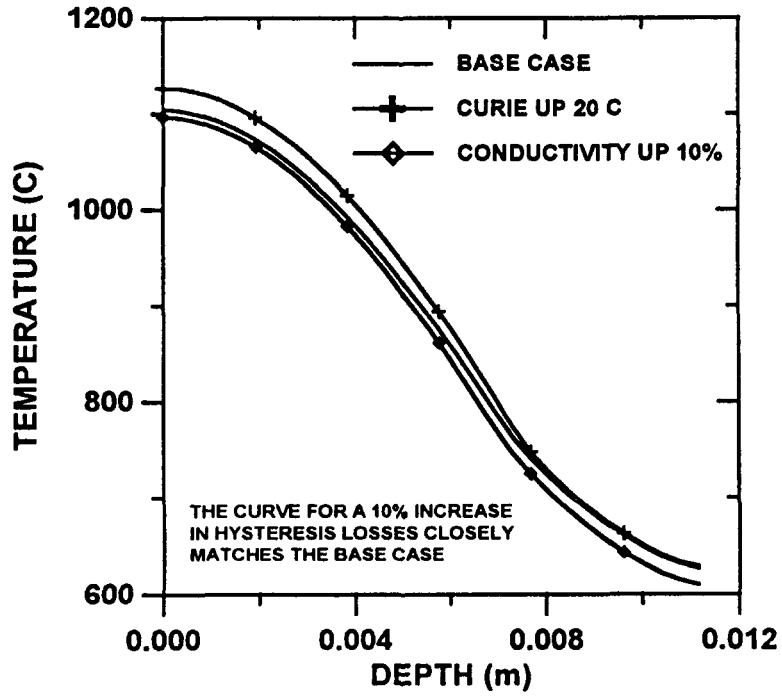

Figure 15. Parametric comparison of temperature profiles at the end of a 5-second induction heating cycle. Results are from the 1-D model for a cylindrical part. Profile for 10% increase in hysteresis loss coincides with base case.

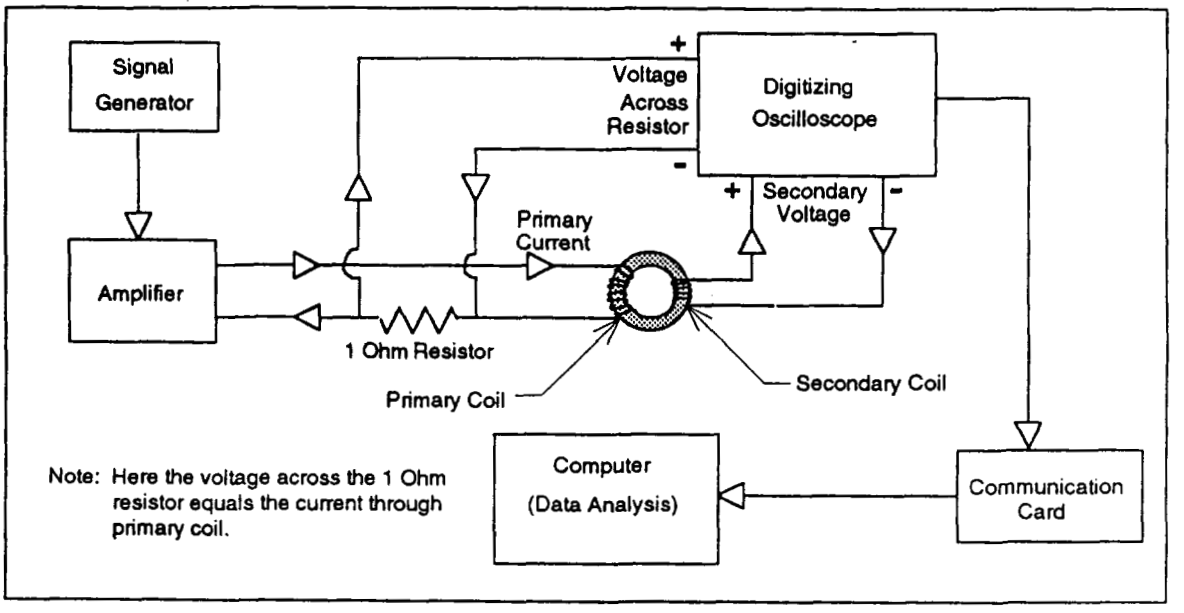

Figure 16. Schematic of system for measuring electromagnetic properties.

Examples of the magnetic characteristics of the 1050 steel that is used in Saginaw's production half-shafts are shown in Figures 17 and 18. The area within the hysteresis loop represents the losses that occur as the magnetic field reverses around the part. This loss contributes to the heating of the part. The slope of the loop represents the magnetic permeability. During the heating process, the temperature of the part increases, and operating frequency of the induction heater changes. Figures 17 and 18 show that both of these effects alter the hysteresis losses in the part. As the frequency increases, the energy losses increase, and as the temperature rises, losses decrease until the material reaches the Curie temperature. Above the Curie temperatures, hysteresis losses no longer contribute to the heating of the part.

Figures 19 and 20 show the magnetic characteristics for two samples of 1050 M steel from two suppliers. The properties are similar at room temperature. As the temperature rises, however, hysteresis losses drop more rapidly in the Inland steel and the permeability is noticeably higher. The more rapid drop in losses indicates that the Inland steel has a lower Curie temperature than the Republic.

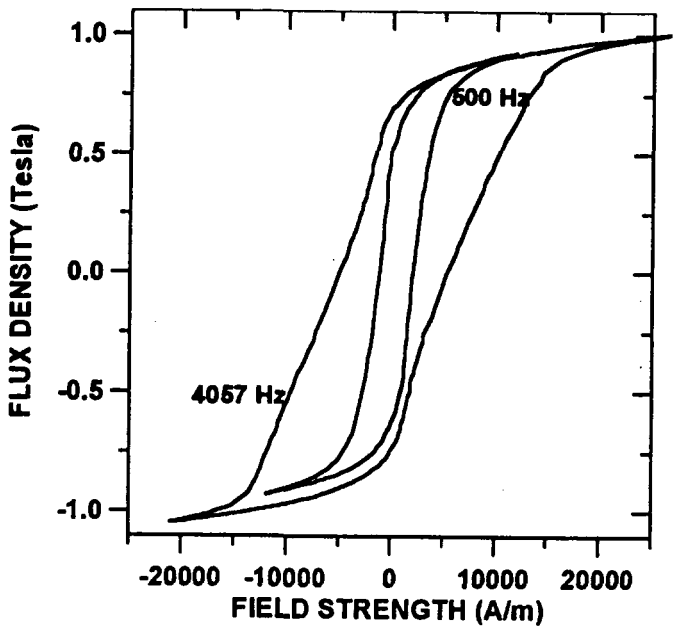

Figure 17. Measured magnetization hysteresis as a function of frequency.

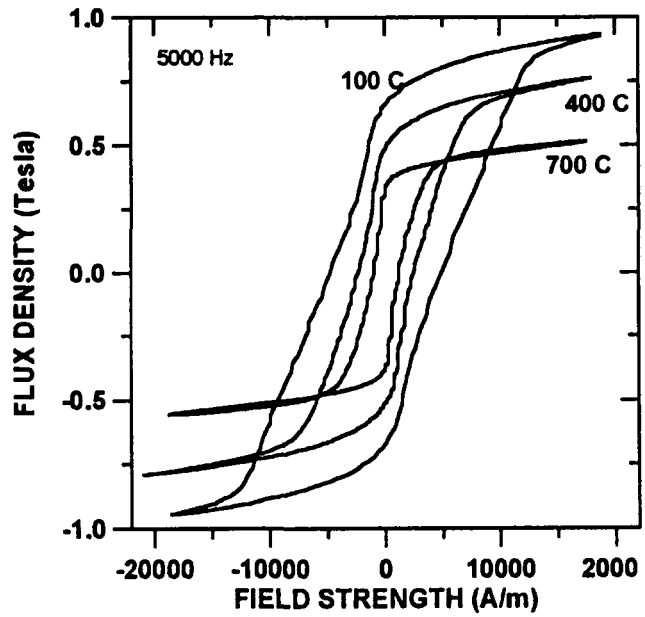

Figure 18. Measured magnetization hysteresis as a function of temperature.

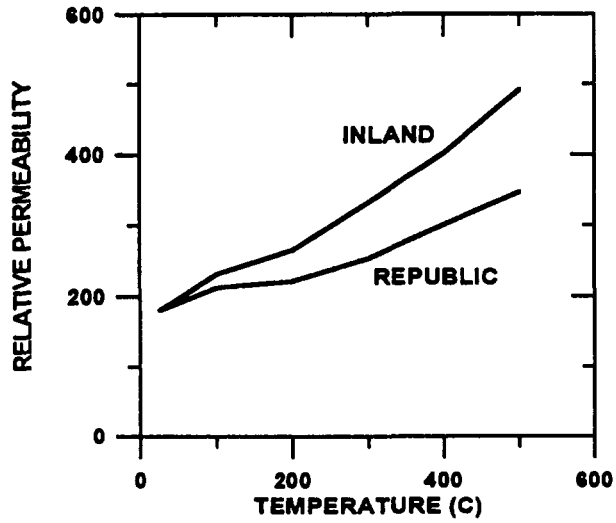

Figure 19. Comparison of measured relative permeability of 1050M steels from two vendors.

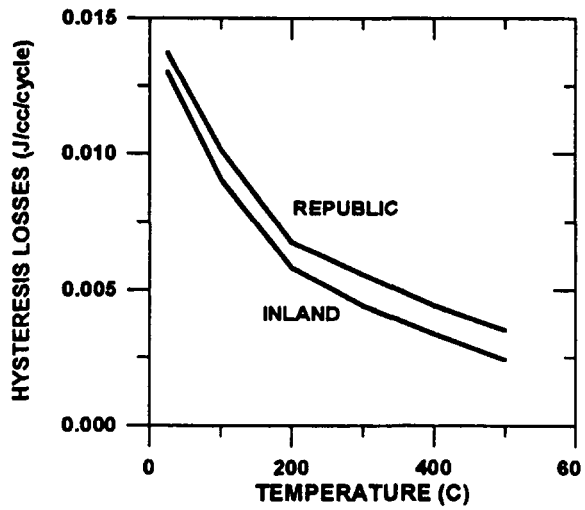

Figure 20. Comparison of measured hysteresis losses of 1050M steels from two vendors.

Specifying the electromagnetic properties for the material is probably impractical for automotive parts production. However, once an induction controller is properly trained, the controller should be able to compensate for the material variations. Using the Curie temperature as an input parameter to the neural-network may make it possible to control the process over a larger manufacturing parameter space. Measuring the Curie temperature with the current system is somewhat inconvenient, but it may be possible to devise a system that will give a measure that is indicative of the Curie temperature. This is one avenue that will be investigated in the next year of this CRADA.

3-D Model Development

While the 1-D model can give useful insights into the dominant parameters in the induction heating process, a full three dimensional model is needed to give practical answers to induction heating problems. For the 3-D model, the coupled electromagnetic and thermal fields that are associated with the induction heating process are being simulated using a combination of the finite element codes; TORO II solves the electromagnetic problem and COYOTE II provides a solution to the thermal problem [Gartling and Hogan, 1994]. The two finite element codes are coupled through the Parallel Virtual Machine (PVM) software which allows the individual codes to be maintained separately and run on one or more CPU's.

The electromagnetic solution determines the volumetric heating in the part that results from resistance heating and hysteresis losses. This heating is used as an input to the thermal model to determine the temperature profile in the part as a function of time. Temperature changes, of course, affect the electromagnetic properties that influence the electromagnetic solution. The time scale for the electromagnetic response ($t_{em} \approx 1/f$) is significantly less than the thermal time scale ($t_{ther} \approx diameter^2/thermal\ diffusivity$). To save on computational time, the thermal problem is accurately solved in time, and the electromagnetic problem is updated periodically as dictated by significant changes in temperature.

Table II provides the basic equations that are used to provide a solution to the induction heating problem. A quasi-static form of Maxwell's equations is used to solve the electromagnetic problem, and Fourier's law is used to solve the thermal problem. The electrical conductivity, thermal conductivity, specific heat and density are all allowed to change with temperature. The magnetic permeability is a function of both the temperature and the magnetic flux density.

Work on the 3-D induction heating computer code has not been completed. Both codes are operational, but work is currently underway to fully couple the codes and to validate the predicted results.

Table II. Governing equations for 3-D model.

ELECTROMAGNETIC EQUATIONS:

$$\nabla \times \left(\frac{1}{\mu} \nabla \times \vec{A} \right) = -\sigma \frac{\partial \vec{A}}{\partial t} - \sigma \nabla \phi$$

$$\nabla \cdot \left(-\sigma \nabla \phi - \sigma \frac{\partial \vec{A}}{\partial t} \right) = 0$$

$$\vec{B} = \nabla \times \vec{A}$$

$$H = \frac{1}{\mu} B$$

$$\vec{J} = \sigma \vec{E} = \sigma \left(-\nabla \phi - \frac{\partial A}{\partial t} \right)$$

$$Q = \vec{J} \cdot \vec{E} + loss$$

THERMAL EQUATION:

$$\rho C \frac{\partial T}{\partial t} = \nabla \cdot (k \nabla T) + Q$$

PROPERTIES:

$\mu = \mu(T,B)$

$\sigma = \sigma(T)$

$\rho C = \rho C(T)$

$k = k(T)$

3-D Test Results

The first full test case for the 3-D model will be a grooved cylinder made of 1050M. The grooved sample is 25.4-mm long by 23.8-mm in diameter with four longitudinal grooves. Induction heating tests have been performed on one of these samples to measure the temperature profile during a heating cycle. Thermocouples were intrinsically welded in holes halfway through the sample at the four locations shown in Figure 21. A slip-ring assembly allowed the part to be rotated during the heating process.

Figure 22 shows the measured temperatures in the part during a 5 second induction heating run. Coil signal measurements indicated that a total energy of about 34.6 kJ went into the part while about 50 kJ went into the coil/part system. The temperature at the surface of the part rose the fastest, but by the end of the heating cycle, the temperature at the base of the groove slightly exceeded the surface temperature. The power to the part that was based on the electrical signature is given in Figure 23. The profile shows the characteristic drop in power as the surface temperature nears the Curie temperature (1436°F). Figure 24 shows the final hardening profile in the part.

Results from this experiment and others will be used to verify the predictions of the 3-D model when it becomes fully operational.

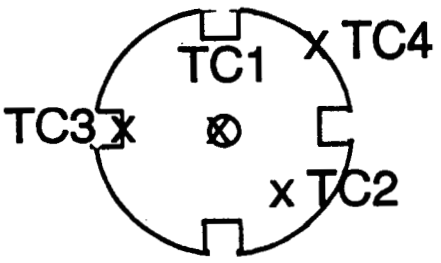

Figure 21. Location of thermocouples in splined test sample.

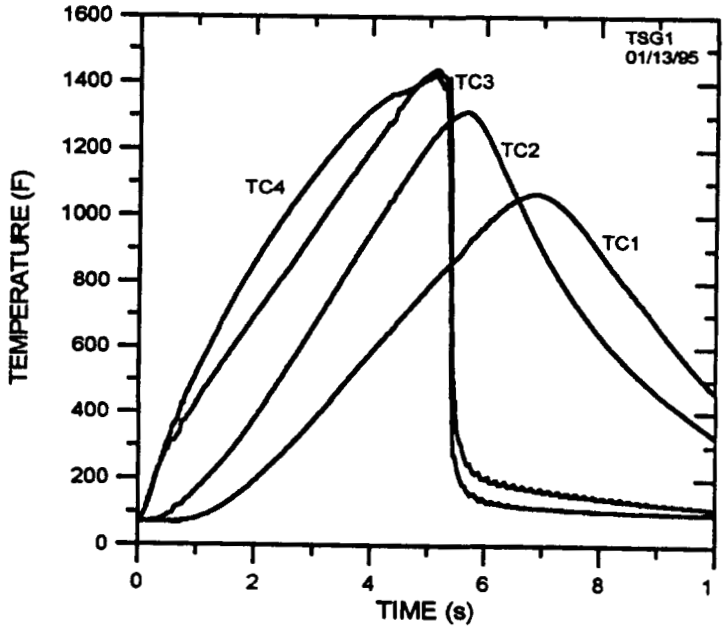

Figure 22. Measured temperatures in splined part during induction heating.

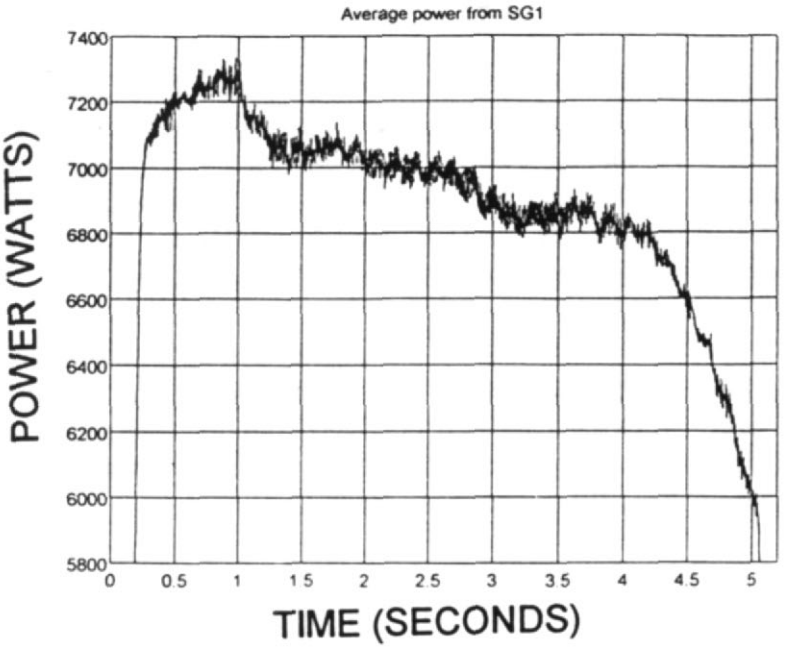

Figure 23. Power to the splined part during induction heating.

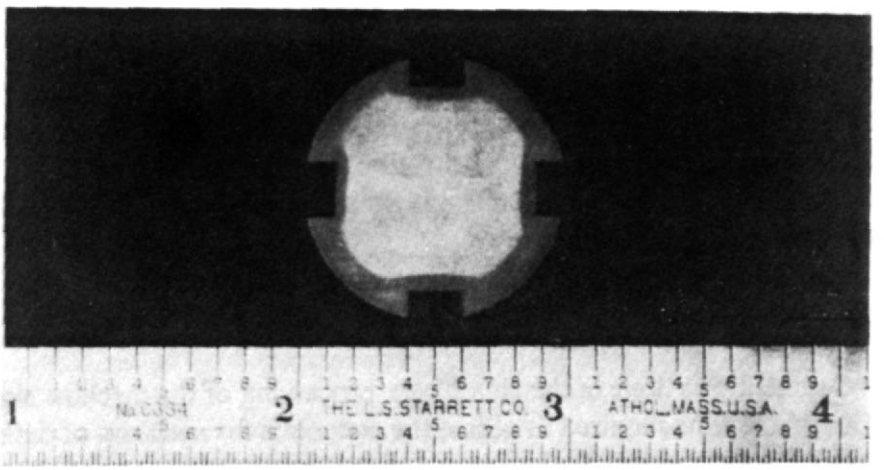

Figure 24. Hardness profile in splined part after induction hardening.

DATA ACQUISITION AND CONTROLLER DEVELOPMENT

The goals for the Data Acquisition/Controller Development Task includes developing a real-time control scheme for the induction hardening process for a complex-geometry production part. So far, the following items have been achieved: identified the pertinent information for real-time on-line control; tested prototype data acquisition and signal processing systems and process control system; developed a monitor/control scheme for simple geometry, single material. Currently, the system is ready to begin implementation at the Saginaw facilities for the Saturn intermediate shafts.

The unique monitor and controller have been successfully demonstrated. Instead of using trial and error to set up the machine for a specific case depth requirement, the operator may now set the power to within a normal specified range, enter the material properties (from the plant's incoming reports) and enter a desired case depth. The controller monitors the energy into the part and into the machine, and determines when the part has obtained the desired case depth.

To achieve this new method of control, several tasks were completed in CRADA Year 2. A model of the system was built for control methodology from the factor space experiments. Neural networks were used to develop the monitor and control scheme, which was demonstrated in June 1994. In July, the monitor was transferred to the Saginaw lab machine, and successfully demonstrated there. Then, a real-time system was designed and built into prototype hardware. This was demonstrated as both a monitor and controller in late 1994. The heat-to-heat material variations and geometry effects on the system model were also evaluated, along with data from scanning runs.

System Model

A system model was developed for the control methodology. The signal processing and data evaluation system was improved for higher fidelity output, basically getting some of the 'noise' out of the system. The necessary experiments for process characterization and neural network training were completed. Experiments were also done for model validation, for both the control model and the first principles model. The extensive workstation calculations for signal processing were eventually replaced by a hardware signal processor.

Neural Network Development

Extensive development was done in the area of pre-processing of the machine signals for input to the neural network. Due to the time required to obtain the endpoints for each run of data, a limited amount of data was available for training. By judiciously choosing the input parameters, a network which generalized relatively well was developed. The input signals investigated included: energy into the workpiece, maximum average power, maximum total resistance, number of seconds of heating after reaching Curie temperature, materials properties (DI and carbon content), and several variations on each of these signals.

A sketch of one of the neural networks investigated is seen in Figure 25. Backpropagation learning was used for this network. Sigmoidal and hyperbolic tangent functions were used for the node transfer functions. Use of linear outputs and various weighted learning schedules were also investigated for this set of data.

Investigation was also done into the use of signals from alternate sensors, including a B-dot sensor, an internal current sensors and a Rogowski coil. These inputs were investigated in conjunction with work being performed in other task areas. (See discussion in Process Characterization Section.)

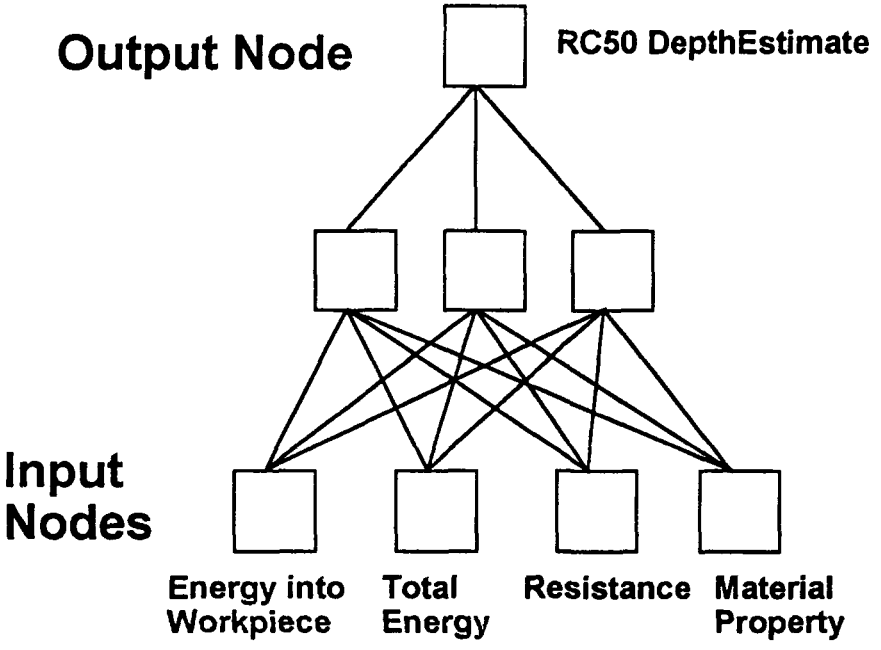

Figure 25. Neural network configuration

Results

For purposes of demonstrating of the technology, it was first desired to show the ability of a neural network to adequately estimate the outcome of an induction run from the electrical signals. From the network development discussed previously, some successful networks were obtained for a simple geometry and a single heat of material. These results are shown in Figures 26 and 27. The points shown in Figure 26 correspond with the data sets that were used to train the network. The solid lines show the RC50 depth that was estimated by the neural net when the training data set was used as the input to the net. Figure 27 shows a comparison between the estimated and measured HRC 50 depth for an independent set of test data (i.e., data that were not used in training the network). The outputs from the given network were able to predict the HRC50 depths to within the manufacturing design tolerances of +/- 0.10mm.

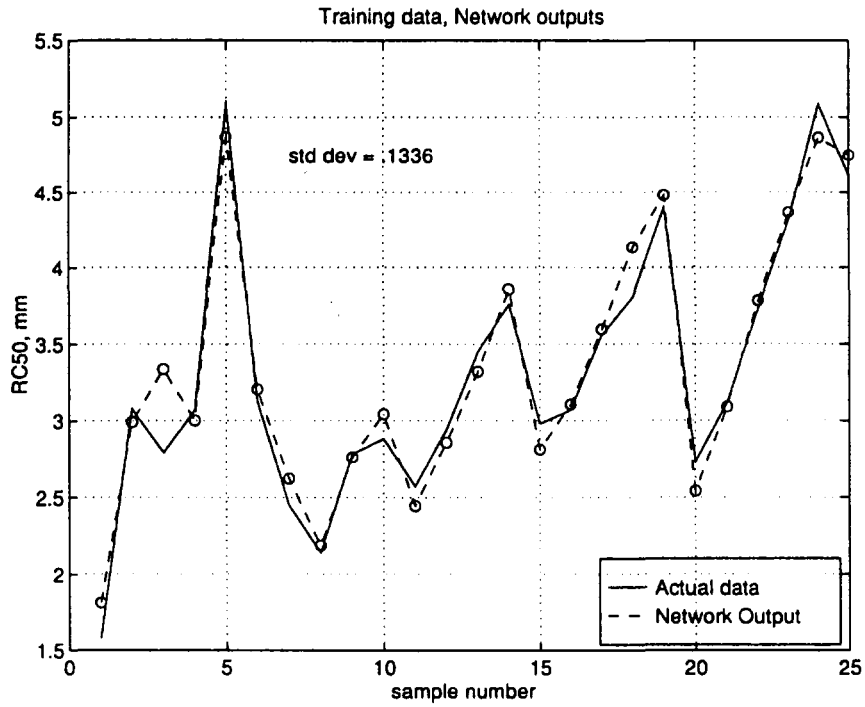

Figure 26. Training the neural network.

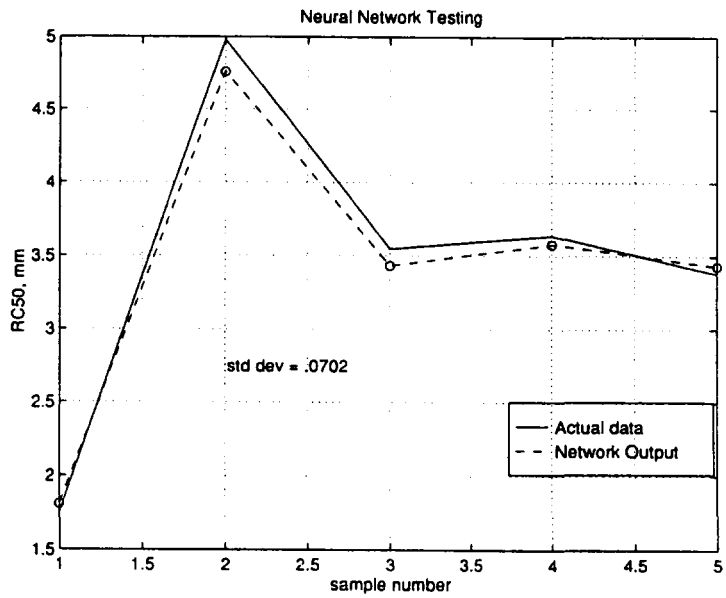

Figure 27. A comparison between measured RC50 depths and neural network estimates for an independent data set.

From a first examination of the experimental data from the material factor space, some general trends can be seen. (See Figures 28 and 29). Notice, however, that in the region of greatest interest, RC50 of 4.0 to 5.0 mm, these trends are not separable enough to form a straightforward or linear relationship between any one measurable feature and the output of RC50 depth. The neural network, which is known for its nonlinear mapping capabilities, is able to couple several of the inputs to map to a reasonable estimate of the output.

The material factor space experiments encompassed a wide range of material properties. The 45 data points from this experiment were used to train a network. Results from the training set are shown in Figure 30. This shows a good mapping of the training data to within an average error of .0704mm. The test set consisted of 6 data points which were not included in the training set. As can be seen in Figure 31, the generalization was fairly good, to an average total error of 0.1240mm. Considering that the best methods for measuring the output data are accurate to only +/-0.1mm, this mapping is good.

Demonstration in Saginaw Lab

The data acquisition system was duplicated in the Saginaw lab on a duplicate production machine by a joint effort of the Saginaw and Sandia participants in June of 1994. The resulting waveforms from the Saginaw machine differed greatly from the waveforms on the machine at the Sandia facility. Data were acquired from this machine for simple and complex geometry parts, and for single shot and scanning modes of operation. Despite the differences in waveform shapes, a neural network of the same architecture and input domains was trained for the Saginaw machine from a small lot of data. Using this newly trained network, a software-based monitor was demonstrated to predict the hardening depth to within the 0.1mm tolerance.

Demonstration of Monitoring and Control

Demonstrations were done separately for both monitor and controllers. The monitor systems were demonstrated at both Sandia and Saginaw in May, June and July, 1994. These monitors were run using software schemes only, which took about 10 minutes to complete computations on a PC. A hardware signal processor was necessary to implement a real-time estimator and controller. A rough prototype of the hardware was in place in August. Due to the format changes in the data, new training data were required for this hardware. A new network was trained, and the real-time controller was successfully demonstrated on the Sandia machine in November. This controller was able to accurately control the machine to achieve a desired RC50 depth to within 0.10mm in a single heat of steel.

Tested and Evaluated Prototype Controllers

Sandia designed the signal processing hardware to replace the extensive calculations done on the host computers. The first rough prototype was built in July, and implemented at Sandia in August. After much development of the electronics and elimination of noise problems, the real-time controller was demonstrated in November. Printed circuit boards were built in January of 1995.

It is important to note that the signal processing hardware is essential for the real-time prototype controllers. Several networks were tested for accurate estimation of the hardness depth. The best systems were able to control the process to 0.10mm. Rough compensation was done for the delay times between the host computer and the machine controllers.

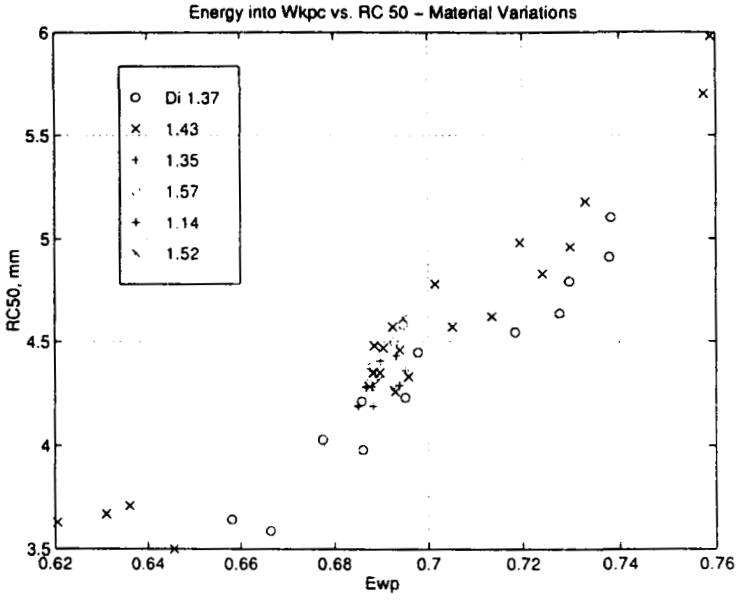

Figure 28. Results from the material factor of space experiment showing the relationship between the energy into the workpiece and the RC50 depth.

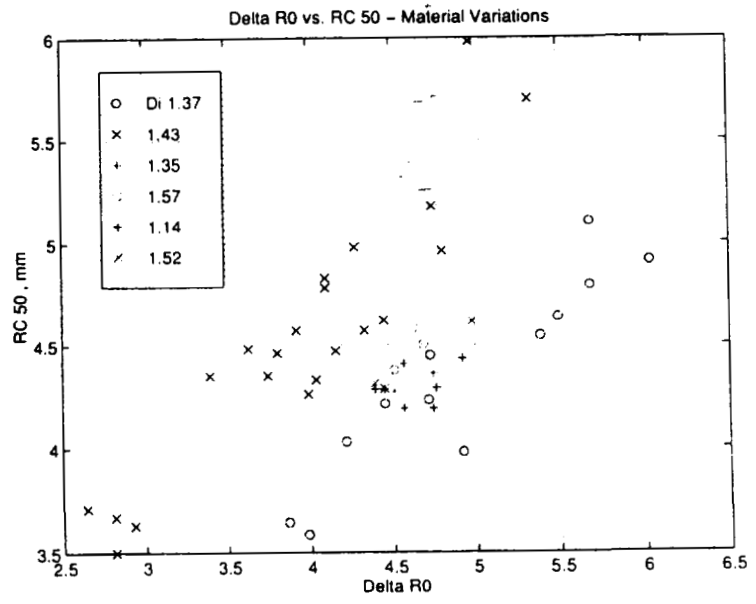

Figure 29. Results from the material factor of space experiment showing the relationship between the change in the overall circuit resistance and the RC50 depth.

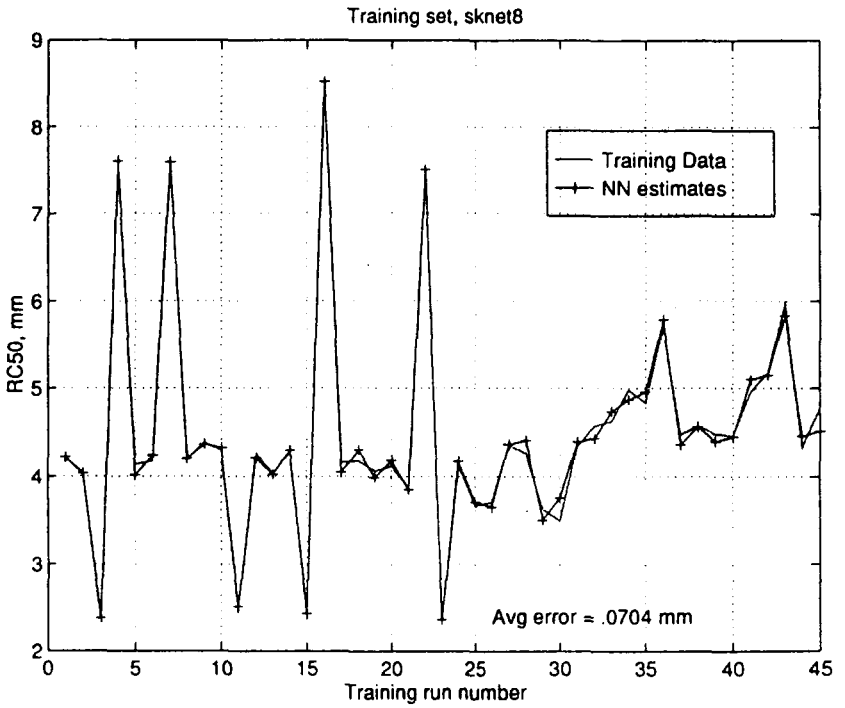

Figure 30. Training of the neural network using the 45 data points generated in the factor of space experiments.

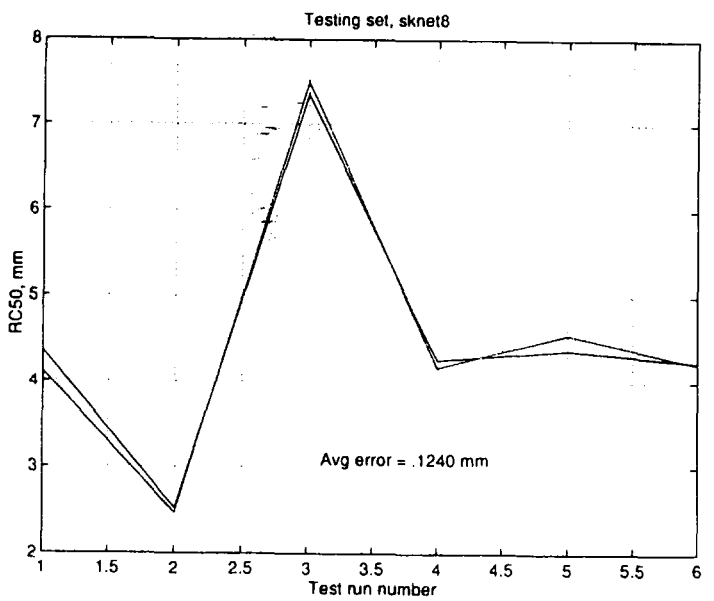

Figure 31. RC50 depth estimated by the neural network trained with the factor of space experiments.

SUMMARY AND CONCLUSIONS

Induction hardening is widely used to provide enhanced strength, wear resistance, and toughness in components made from medium and high carbon steels. Currently, use of the process is limited because of several factors. These factors include: (1) the lack of closed-loop process control, (2) unidentified process and material variations cause continual adjustment of the process parameters, and (3) coil and process development is by trial and error. To overcome these limiting factors, it is necessary to develop an improved understanding of process fundamentals and material/process interactions. It is also necessary to develop a robust control system that can compensate for changes in process variables.

A multidisciplinary team from Sandia National Laboratories and Delphi Saginaw Steering Systems (a wholly owned subsidiary of General Motors) is investigating the induction hardening process under a Cooperative Research and Development Agreement (CRADA). The program consists of four tasks: (1) Process Characterization, (2) Materials Characterization, (3) Computational Modeling, and (4) Data Acquisition and Control. Over the past year, advances have been made in each of these areas that will further our ultimate goal of improving the industrial application of induction hardening of materials. The primary goal for the first year of this program was to establish a technical base in each of these areas that allowed us to understand the induction heating process, and to identify the best approach to control the process in a laboratory environment. The second year of this program was dedicated to implementing this knowledge to control the induction heating process in the laboratory enviroment, and to begin developing the hardware and software needed for control on the factory floor. In the third and final year of this program, the control system will be introduced to the factory floor and the knowledge and computational tools developed in this program will be fully transferred to Saginaw.

Accomplishments in each of the task areas in this, the second year of the CRADA can be summarized as follows:

Process Characterization

- Characteristic process signals were evaluated across heat-to-heat variations within material supplied by one vendor. While no clear cut correlations were found, the use of ideal diameter and carbon content were useful inputs for the neural network based controller.
- Characteristic process signals were evaluated across a range of geometry variations. For both right circular cylinders of various diameters and splined-end bars, variations in the absolute values of the signals were observed but the signal characteristics were identical. These variations required no changes to the signal processing or control algorithms.
- Alternative coil current monitoring approaches were developed and evaluated. B-dot probes mounted on the coil and the internal current sensor of the machine can both be used for control purposes. However, the absolute values of the characteristic signals produced when using these sensors cannot be correlated with to the fundamentals of the process.

- Single shot and scanning process data from different power supplies were studied at the Saginaw Induction lab. The characteristic signals were consistent across power supplies. Scanning processes will require different control algorithms.

Materials Task

- The hardenability/quench severity analysis has been completed. The results of this analysis indicate that the induction hardening process generally operates in the heating limited regime. As a result, the characteristics of the formation of austenite are of primary importance in this process. Since the process is controlled by on-heating behavior, process controls based on energy input are physically appropriate.
- A jointly generated materials database has been established for a large number of stockpiled heats. This stockpile and database is being expanded and provides valuable information on real heat-to-heat variation.
- A new method for characterizing the austenitization kinetics of hypoeutectoid steels has been developed. Although this method has not been fully refined, differences between heats have been observed. It is believed that this approach will yield materials characteristics which are applicable to process control philosophies.

Modeling Task

- A thermal analysis validated the system-model estimated power distribution to the coil and workpiece. Calorimetry work showed that the electrical signal analysis that is used in controlling the induction heater can estimate power to the workpiece to within 3%.
- Magnetic property variations were evaluated among material suppliers. Variations in magnetic properties were small for 1050M steel at room temperature. At higher temperatures, however, variations were significant, and they would lead to differences in the induction heating profile. A 1-D induction heating model showed that the sensitivity to Curie temperature variations dominates the induction heating process.
- Coding for the 3-D induction heating model was completed. The coupled electromagnetic and thermal fields that are associated with the induction heating process are simulated using a combination of the finite element codes; TORO II solves the electromagnetic problem and COYOTE II provides a solution to the thermal problem. The two finite element codes are coupled through the Parallel Virtual Machine (PVM) software which allows the individual codes to be maintained separately and run on one or more CPU's. Validation of the code is still pending.
- Test data was generated to validate the 3-D model. Temperature profiles on a splined shaft were obtained during an induction-heating and quench cycle. The electrical signature was also measured during the heating cycle to give an estimate of the power to the part and coil. Together, this information will be used to validate the 3-D model results.

Data Acquisition and Control

- A prototype hardware signal processor was designed and built to speed computations. The signal processing hardware was required for real-time control.
- A first generation neural network controller was demonstrated at Sandia. Application of intelligent control algorithms has led to the development of a closed-loop process controller that controls the HRC 50 case thickness to $\pm$ 0.1 mm for the combination of one material and one geometry in a single-shot process.
- A neural network controller was also sucessfully demonstrated at the induction laboratory at Delphi Saginaw.
- Data streams were collected for scanning induction systems at Saginaw to explore the possibility of controlling a wider variety of induction machines with a neural network system.

These accomplishments have positioned the program at a point where the third year goal of introducing the neural-network induction control system on the factory floor at Delphi Saginaw is achievable. Further work in computational modeling and materials characterization in the third and last year of the CRADA will also improve the application and understanding of this important idustrial heat treating process.

REFERENCES

Adkins, D. R., B. K. Damkroger, C. A. Frost, P. M. Kahle, J. B. Kelley, G. A. Knorovsky, C. V. Robino, A. J. Russo, R. D. Skocypec, and S. L. Stanton, 1994, "Intelligent Systems for Induction Hardening Processes," Sandia National Laboratories Report No. SAND94-1471, Sandia National Laboratories, Albuquerque, NM.

Ashby, M. F., and K. E. Easterling, 1984, "The Transformation Hardening of Steel Surfaces by Laser Beams - I. Hypoeutectoid Steels". *Acta Metall.* Vol. 32, No. 11, pp. 1935-1948.

Davies, J. and P. Simpson, 1979, *Induction Heating Handbook*, McGraw-Hill, London.

Frost, C. A., P. M. Kahle, S. L. Stanton, D. R. Adkins, A. J. Russo, J. B. Kelley, G. A. Knorovsky, 1994, "A Method and Apparatus to Measure Power Delivered to an Inductively Heated Part", Technical Advance Disclosure, SD 5455, Sandia National Laboratories, Albuquerque, NM, May 18, 1994.

Gartling, D. K., and Hogan, R. E., 1994, "Coyote II - A Finite Element Computer Program For Non-Linear Heat Conduction Problems, Part II, Users Manual", SAND94-1179, Sandia National Laboratories, Albuquerque, NM

Hassell, P. A., and Mordwinkin, G., 1986, *Industrial Heating*, Vol 53, No. 12, pp. 17-20.

Hassell, P. A., 1994, "Potential of Monitoring Induction Heating in Real Time", Industrial Heating, Vol 61, No. 1, pp. 42-45.

Kern, R. F., and M. E. Suess, 1979, *Steel Selection, A Guide For Improving Performance and Profits*, John Wiley and Sons, New York, pp. 212-216.

Knorovsky, G. A., C. V. Robino, B. K. Damkroger, and J. B. Kelley, 1995, "Induction Hardening Variation Inferred from Quantitative Hardenability Theory", *In Press.*

Martin, D. L., and Wiley, F. E., 1956, "Induction Hardening of Plain Carbon Steels: A Study of the Effect of Temperature, Composition, and Prior Structure on the Hardness and Structure After Hardening", Trans. ASM, Vol 34, pp. 351-396.

Mordwinkin, G., A. L. Vaughn, and P. Hassell, 1986. "New Induction QC Method Uses Eddy Current Principle" *Heat Treating*, Vol 18, No. 11, pp. 34-38.

Semiatin, S. L., and D. E. Stutz, 1986, *Induction Heat Treatment of Steel*, American Society For Metals, Metals Park, OH.

Storm, J. M., and M. R. Chaplin, 1987, "Induction Gear Hardening by the Dual Frequency Method", *Heat Treating*, Vol 19, No. 6, pp. 30-35.

Tudbury, C. A., 1960, *Basics of Induction Heating*, Vol 1, John F. Rider, Inc., New York, Reprinted By University Microfilms International.

Verhoeven, J. D., H. L. Downing, and E. D. Gibson, 1986, "Induction Case Hardening of Steel", Journal of Heat Treating, Vol 4, No. 3, pp. 253-264.

Zinn, S. and S. L. Semiatin, 1988, *Elements of Induction Hardening*, ASM International, Metals Park, OH.

Distribution

1	R. Peavey, DOE/DP	
1	J. Farago, GM, Saginaw Division	
1	D. M. Hitz, GM, Saginaw Division	
1	R. P. Hoppe, GM, Saginaw Division	
1	D. D. Rogers, GM, Saginaw Division	
1	MS0337	A. D. Romig, 1800
1	MS0340	M. J. Cieslak, 1831
1	MS0340	G. A. Knorovsky, 1831
1	MS0340	C. V. Robino, 1831
1	MS0341	J. L. Jellison, 1833
1	MS0501	P. M. Kahle, 2338
1	MS0501	S. M. Kohler, 2338
1	MS0501	S. L. Stanton, 2338
1	MS0501	J. Spooner, 2338
1	MS0509	R. D. Andreas, 2300
1	MS0827	A. J. Russo, 1511
1	MS0827	D. Gartling, 1511
1	MS0835	D. R. Adkins, 1513
1	MS0835	R. D. Skocypec, 1513
1	MS0841	P. J. Hommert, 1500
1	MS1134	B. K. Damkroger, 1833
1	MS1134	J. B. Kelley, 1833
1	MS1134	F. J. Zanner, 1833
1	MS1153	M. T. Buttram, 1248
1	MS1153	F. J. Zutavern, 1248
1	MS1190	D. L. Cook, 1200
1	MS1380	B. H. Vandomelen, 4200
1	MS1380	K. W. Bieg, 4202
1	MS1380	D. W. Larson, 4202
1	MS1380	M. Monson, 4202
1	MS9018	Central Technical Files, 8523-2
5	MS0899	Technical Library, 13414
1	MS0619	Print Media, 12615
2	MS0100	Document Processing for DOE/OSTI, 7613-2
3	MS0161	Patents and Licensing Office, 11500

THIS PAGE INTENTIONALLY LEFT BLANK